

## **General Disclaimer**

### **One or more of the Following Statements may affect this Document**

- This document has been reproduced from the best copy furnished by the organizational source. It is being released in the interest of making available as much information as possible.
- This document may contain data, which exceeds the sheet parameters. It was furnished in this condition by the organizational source and is the best copy available.
- This document may contain tone-on-tone or color graphs, charts and/or pictures, which have been reproduced in black and white.
- This document is paginated as submitted by the original source.
- Portions of this document are not fully legible due to the historical nature of some of the material. However, it is the best reproduction available from the original submission.

NASA CR-144763

RQT

DTM-71-3

Final Report

for

# Heat Pipe Heat Rejection System

Contract NAS5-21523

Prepared for

Goddard Space Flight Center  
Greenbelt, Maryland 20771



***dynatherm*** CORPORATION

Cockeysville, Maryland 21030

(NASA-CR-144763) HEAT PIPE HEAT REJECTION  
SYSTEM Final Report (Dynatherm Corp.,  
Cockeysville, Md.) 53 p HC \$4.50 CSCI 20M

N76-26421

G3/34

Unclas  
42294



## ABSTRACT

A prototype of a battery heat rejection system was developed which uses heat pipes for more efficient heat removal and for temperature control of the cells. The package consists of five (5) thermal mock-ups of 100 amp-hr prismatic cells. Highly conductive spacers fabricated from honeycomb panels into which heat pipes are embedded transport the heat generated by the cells to the edge of the battery. From there it can be either rejected directly to a cold plate or the heat flow can be controlled by means of two (2) Variable Conductance Heat Pipes.

The thermal resistance between the interior of the cells and the directly attached cold plate was measured to be  $0.08^{\circ}\text{F}/\text{Watt}$  for the 5-cell battery. Compared to a conductive aluminum spacer of equal weight the honeycomb/heat pipe spacer has approximately one-fifth of the thermal resistance. In addition, the honeycomb/heat pipe spacer virtually eliminates temperature gradients along the cells.

The Variable Conductance Heat Pipes are effective in reducing the influence of varying sink conditions on the cell temperature. During testing the sink temperature was varied between  $-4$  and  $+68^{\circ}\text{F}$  with a corresponding cell temperature fluctuation of less than  $25^{\circ}\text{F}$ . For applications where the sink temperature is very stable however, the best control of the cell temperature is achieved when the battery is interfaced directly with a cold plate.

## FOREWORD

This is a Technical Summary Report issued under Contract NAS5-21523. The report describes the design, fabrication, and testing of a Prototype Heat Pipe Heat Rejection and Temperature Control System for Spacecraft Batteries. The program was administered by the Goddard Space Flight Center, Greenbelt, Maryland. Mr. S. G. McCarron was the NASA technical officer.

The work was completed by Dynatherm Corporation, Cockeysville, Maryland, under the direction of Mr. Edward Kroliczek. Technical contributors were Messrs. Mike Kreitz, Ted Zarnoch, and James Liles.



## TABLE OF CONTENTS

	<u>Page</u>
1. PROGRAM OBJECTIVE AND SUMMARY . . . . .	1
2. DESIGN DESCRIPTION . . . . .	5
2.1 Battery Cell Thermal Mock-Up . . . . .	5
2.2 ISOPAC Panels . . . . .	6
2.3 Variable Conductance Heat Pipes . . . . .	12
2.4 Pressure Retention Plates . . . . .	19
2.5 Simulated Spacecraft Cold Plate . . . . .	19
3. THERMAL PERFORMANCE TESTS . . . . .	21
3.1 ISOPAC and Simulated Cold Plate . . . . .	21
3.2 ISOPAC Panel, Battery Thermal Mock-Up and Simulated Cold Plate . . . . .	25
3.3 Testing of Complete Prototype of Battery Heat Pipe Heat Rejection System . . . . .	28

APPENDIX A

APPENDIX B

## 1. PROGRAM OBJECTIVE AND SUMMARY

Heat removal from prismatic Ni-Cd cells employed in space applications has always been accomplished by conduction through the cell matrix and controlled dissipation to the ultimate heat sink. Heat produced within the cell assemblies raises the temperature of the cell interior and must eventually escape by conduction to the exterior walls or to the electrical terminals. The inherently low thermal conductivity of the cell structure gives rise to substantial temperature gradients. As the demand for larger capacity cells and battery systems develops, this problem can no longer be ignored. Means must be provided for better thermal coupling between the sources of heat and the ultimate sink. Furthermore, means must be provided to regulate the flow of heat to the sink in order to minimize the source temperature swing.

The objective of this program has been to develop and demonstrate a Prototype Heat Pipe Heat Rejection System for Ni-Cd batteries which is capable of:

- Efficiently removing 125 watts (25 watts/cell)
- Maintaining the internal cell temperature in the range of  $-4^{\circ}\text{F}$  to  $+68^{\circ}\text{F}$  under all typical charge and discharge conditions.
- Restraining the cell case dimensional excursions resulting from internal cell pressures in the range of 5 psia to 40 psia.
- A mission life greater than 20,000 hours.

In support of the heat rejection system demonstration, a thermal mock-up of a battery consisting of five (5) 100 amp-hr prismatic Ni-Cd cells has also been fabricated. A liquid cooled heat sink has been provided which is capable of simulating the cold plate of a spacecraft environmental control system.

The Prototype Battery Heat Pipe Heat Rejection System which was developed under this contract is shown in the photograph, Figure 1-1, and schematically in Figure 1-2. It consists primarily of two independent heat removal subsystems. The "ISOPAC" cell separators constitute the primary heat removal subsystem. The "ISOPAC" panels, containing small ammonia filled heat pipes, are inserted between individual adjacent cells (i.e., mock-ups) to efficiently remove the heat to an intermediate cold plate. This intermediate cold plate constitutes the evaporator section of the Variable Conductance Thermal Control Heat Pipe Subsystem. This second subsystem consists of two (2) variable conductance heat pipes with methanol as the working fluid and argon gas as the noncondensable. The thermal control heat pipes regulate the amount of heat to be transported to the spacecraft cold plate by reacting to changes in the battery heat input or the spacecraft cold plate temperature.

The overall thermal resistance of the mock-up battery which consisted of five (5) cells and six (6) ISOPAC panels was measured to be  $0.082^{\circ}\text{F}/\text{Watt}$  when heat sinked directly with a cold plate. The addition of the variable conductance heat pipes increases that resistance significantly, but the effect of sink temperature fluctuations is attenuated by a factor of 2.5. Heating the gas storage reservoirs of the variable conductance heat pipes provides attenuation of sink fluctuation by a factor of five and a feedback system could afford absolute temperature control.

The initial testing of the Heat Pipe Heat Rejection System conducted at Dynatherm Corporation utilized the battery thermal mock-up. Upon delivery to GSFC, the simulated battery cells will be replaced with actual 100 amp-hr Ni-Cd cells for verification testing of the heat rejection system.

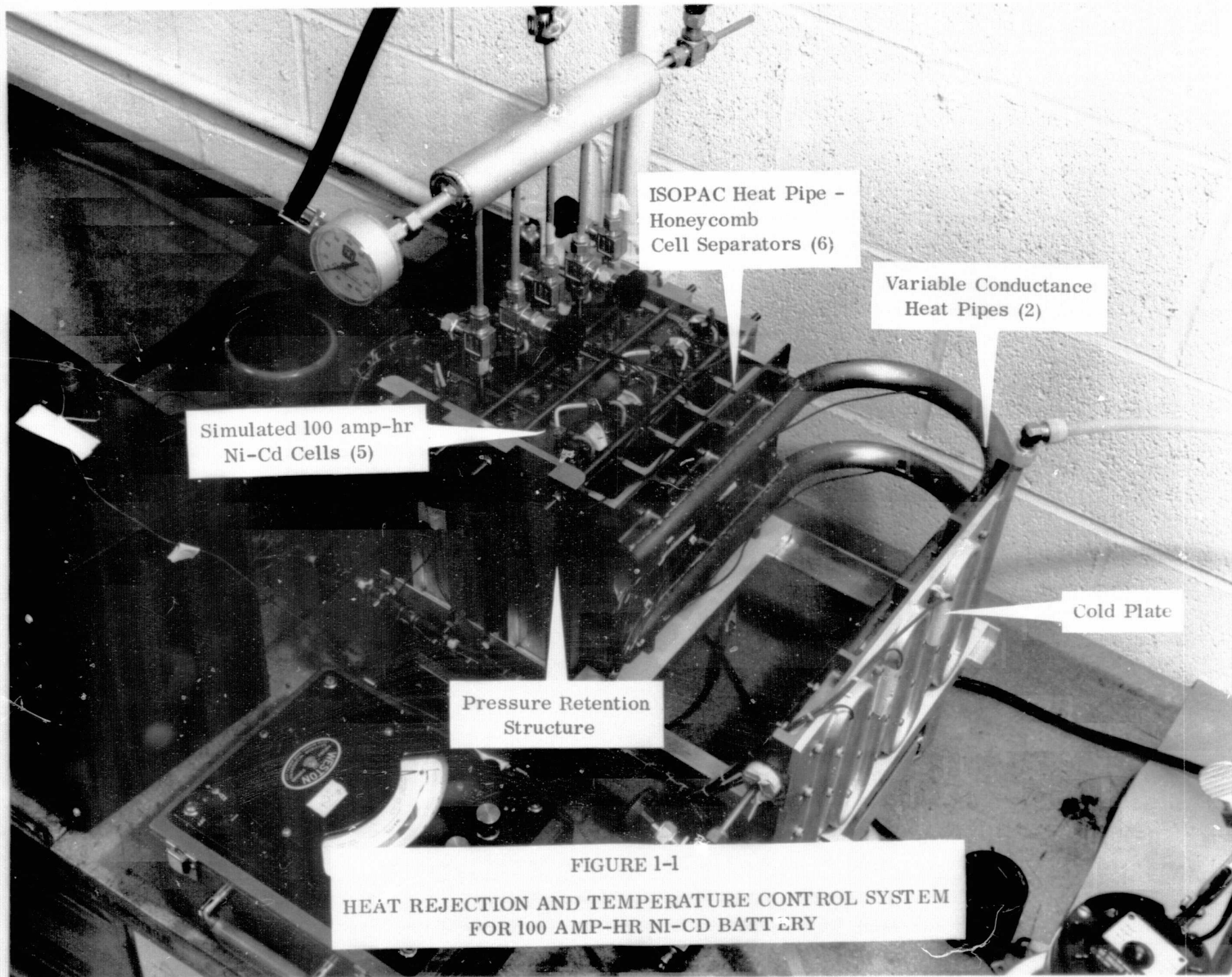


FIGURE 1-1  
HEAT REJECTION AND TEMPERATURE CONTROL SYSTEM  
FOR 100 AMP-HR NI-Cd BATTERY

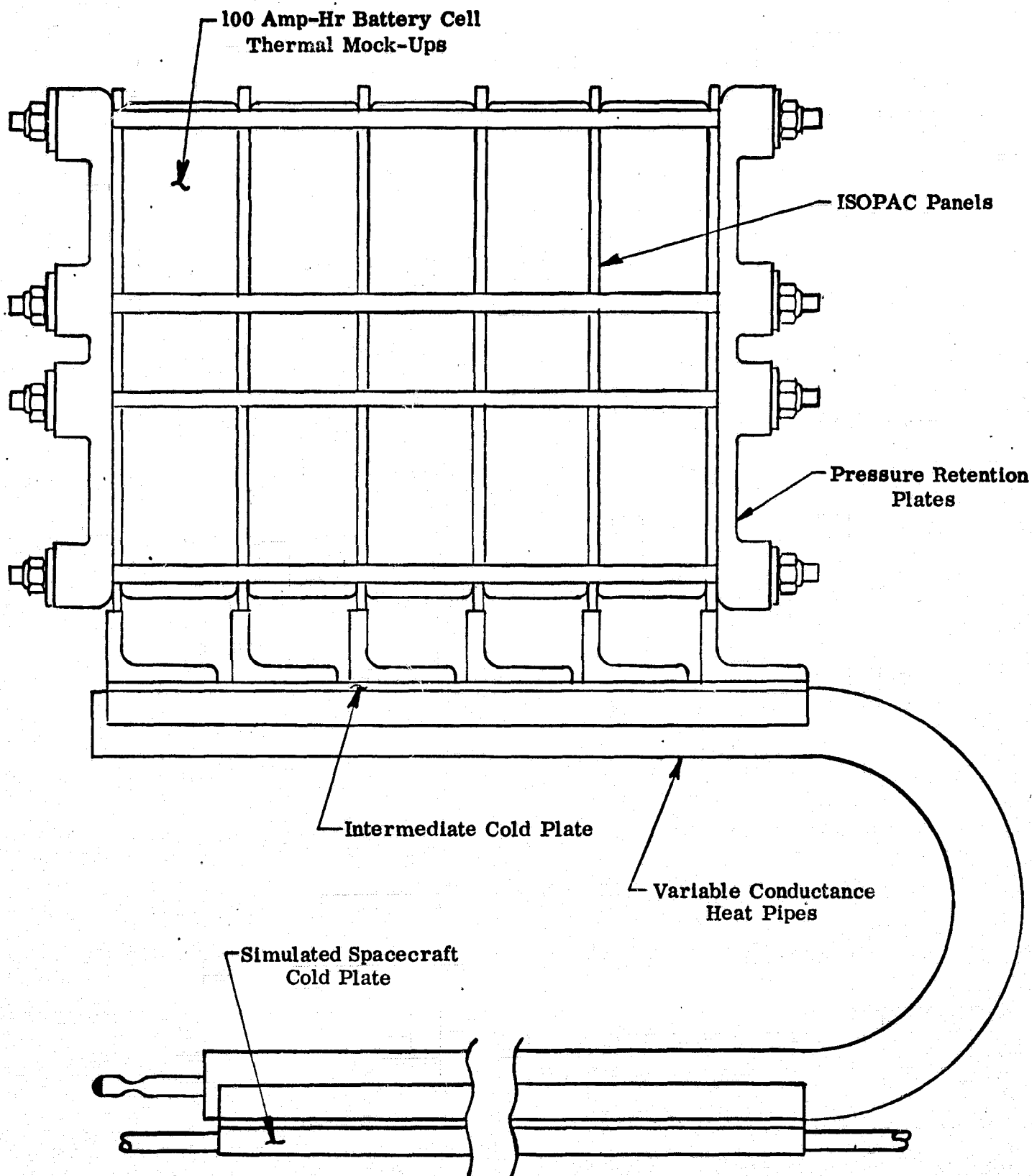


FIGURE 1-2. PROTOTYPE BATTERY HEAT REJECTION SYSTEM

## **2. DESIGN DESCRIPTION**

The Prototype Battery Heat Rejection System which evolved from this program is shown in Figures 1-1 and 1-2. It consists of the following basic components:

- (a) Five (5) thermal mock-ups of 100 amp-hr Ni-Cd cells which are constructed with GE 100 amp-hr prismatic cases and physically interchangeable with a typical five cell Ni-Cd battery pack.
- (b) Six (6) heat pipe panels (Dynatherm "ISOPAC") to remove heat from between the stacked cells. These panels incorporate the required electrical insulation to isolate the cells relative to each other.
- (c) Two (2) variable conductance heat pipes. These heat pipes serve as interfacing elements between the battery pack and the simulated spacecraft cold plate to reduce temperature fluctuations of the cells.
- (d) Two (2) pressure retention plates to minimize cell deflection during the charge-discharge pressure cycles. Sufficient strength has been provided to avoid loss of thermal contact.
- (e) A simulated spacecraft cold plate and a liquid circulation loop capable of maintaining the sink temperature at any selected point within the range of  $-4^{\circ}\text{F}$  to  $+68^{\circ}\text{F}$ .

### **2.1 Battery Cell Thermal Mock-Up**

In order to perform the initial in-house testing of the developed Prototype Battery

Heat Rejection System, it was necessary to design and fabricate a five-cell thermal mock-up of a 100 amp-hr Ni-Cd battery. The thermal mock-up's exterior dimensions are identical to the prismatic cell chosen by NASA for this application. The effective thermal conductance of the mock-up closely reproduces that of a typical Ni-Cd cell in two dimensions.

The battery thermal mock-up basically consists of five (5) actual GE 100 amp-hr stainless steel cell cases, each fitted with an electrically powered aluminum heater block (see Figure 2.1-1). The cell case, as procured from GE, consists of a 7.5" x 7.5" x 1.5" open-ended container constructed of 0.032" thick 304L stainless steel. A heater block assembly was fabricated by uniformly routing resistive heater wire throughout a 6061 aluminum plate. The heater block assembly was then bolted directly to a 304L stainless steel end cap and inserted into the cell case prior to seam welding. The case end has electrical heater wire feed-through provisions, in addition to a bulkhead fill tube for filling and pressurizing the welded assembly. The case end cap also provides thermocouple insertion holes through which temperature instrumentation can penetrate the interior of the cell. The gap within the thermal mock-ups was initially filled with distilled water ( $k = 0.3 \text{ Btu/Hr-Ft-}^{\circ}\text{F}$ ) for the in-house testing of the system. The combination of a low conductivity fluid (water) in the gap between the high-conductivity aluminum heater block yields an effective cell thermal conductivity of  $1.0 \text{ Btu/Hr-Ft-}^{\circ}\text{F}$ . By varying the type of fluid in the gap, a range of effective cell conductivities can be investigated.

## 2.2 ISOPAC Panels

Because of the significant heat generation and removal problem inherent to the operation of large battery systems, a new concept called ISOPAC has been evolved.

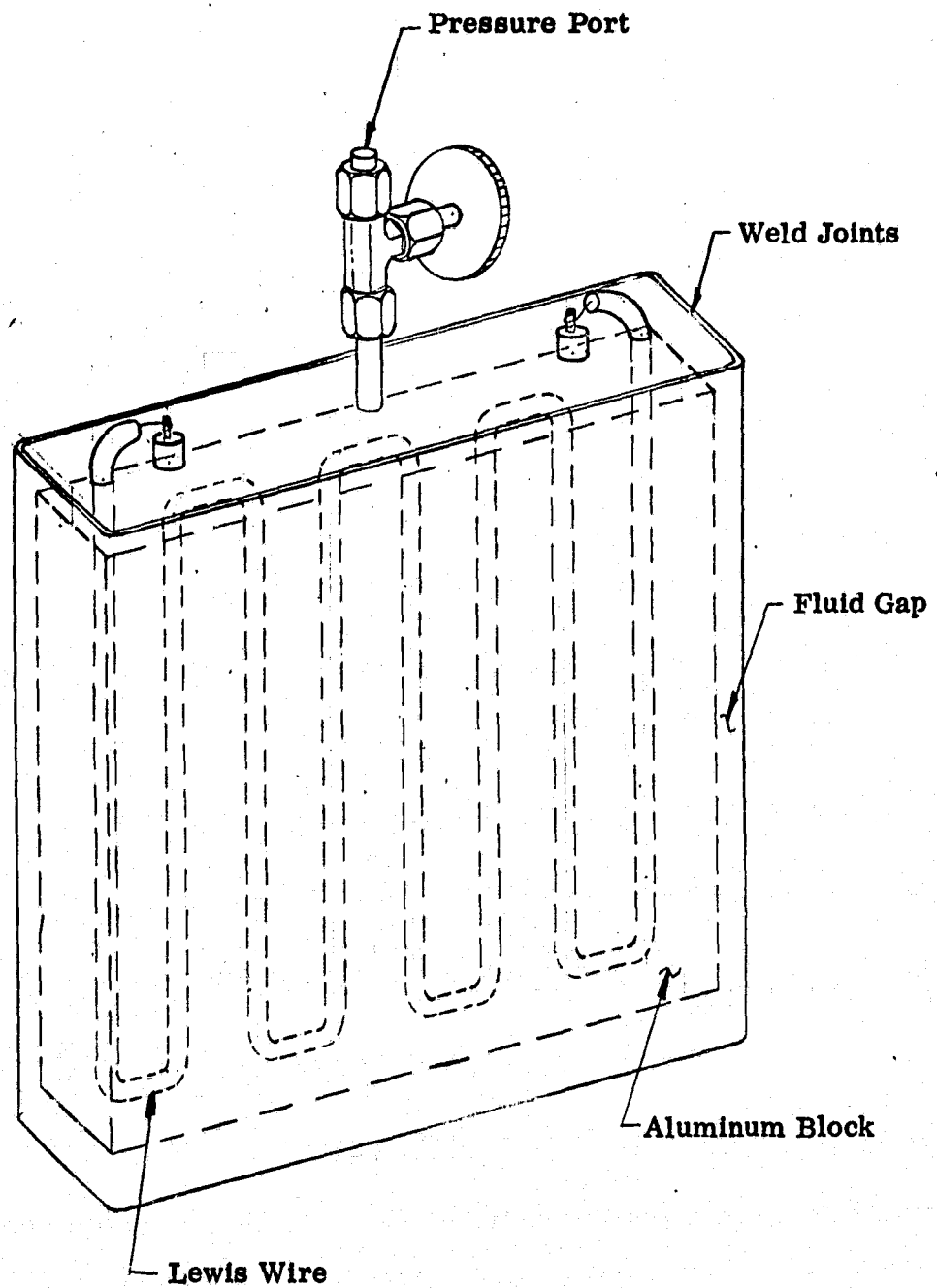


FIGURE 2.1-1  
BATTERY CELL THERMAL MOCK-UP



Figure 2.2-1 shows the ISOPAC panel as employed in the Prototype Battery Heat Rejection System. It consists of a thin (0.160"), lightweight honeycomb structure into which eight (8) aluminum heat pipes have been embedded. At the evaporator section the round 6061 aluminum tubing, from which the heat pipes were fabricated, was machined flat on two surfaces to facilitate their bonding into the honeycomb sandwich. The aluminum honeycomb material of 1/8" cell size fills the space between adjacent heat pipes. The machined heat pipes are charged with ammonia prior to pinch-off and seal welding. The heat pipes and honeycomb material are bonded between 0.020" thick 6061 aluminum face sheets with 0.125" edge members stiffening the entire structure. As shown in Figure 2.2-1, the heat pipes are bent 90° such that the condenser section runs parallel to the narrow edge of the cell. The entire condenser section of each heat pipe is bonded into an aluminum "boot" to improve the heat transfer.

The ISOPAC panel is placed between two adjacent cells and then mechanically attached to the heat sink. Each ISOPAC panel is required to transport 25 watts, meaning that each of the eight ammonia heat pipes is responsible for approximately 3 watts under normal operating conditions. Tests with individual heat pipes have shown a transport capability of 4.5 watts, indicating that a failure of two heat pipes in a single ISOPAC panel would not adversely effect the transport capability of the panel. The design parameters of the ISOPAC panels are summarized in Table 2.2-1. An analytical performance comparison between the ISOPAC panel and solid magnesium conductive spacers is given in Figure 2.2-2. The comparison was made on the basis of uniform heat input from the cells. The plotted thermal resistance includes the  $\Delta T$ 's within both "legs" of the "L" shaped structure and an interface conductance of 500 Btu/Hr-Ft<sup>2</sup>-°F between the short leg of the "L" and an "ideal" cold plate. It should be pointed out that in addition to

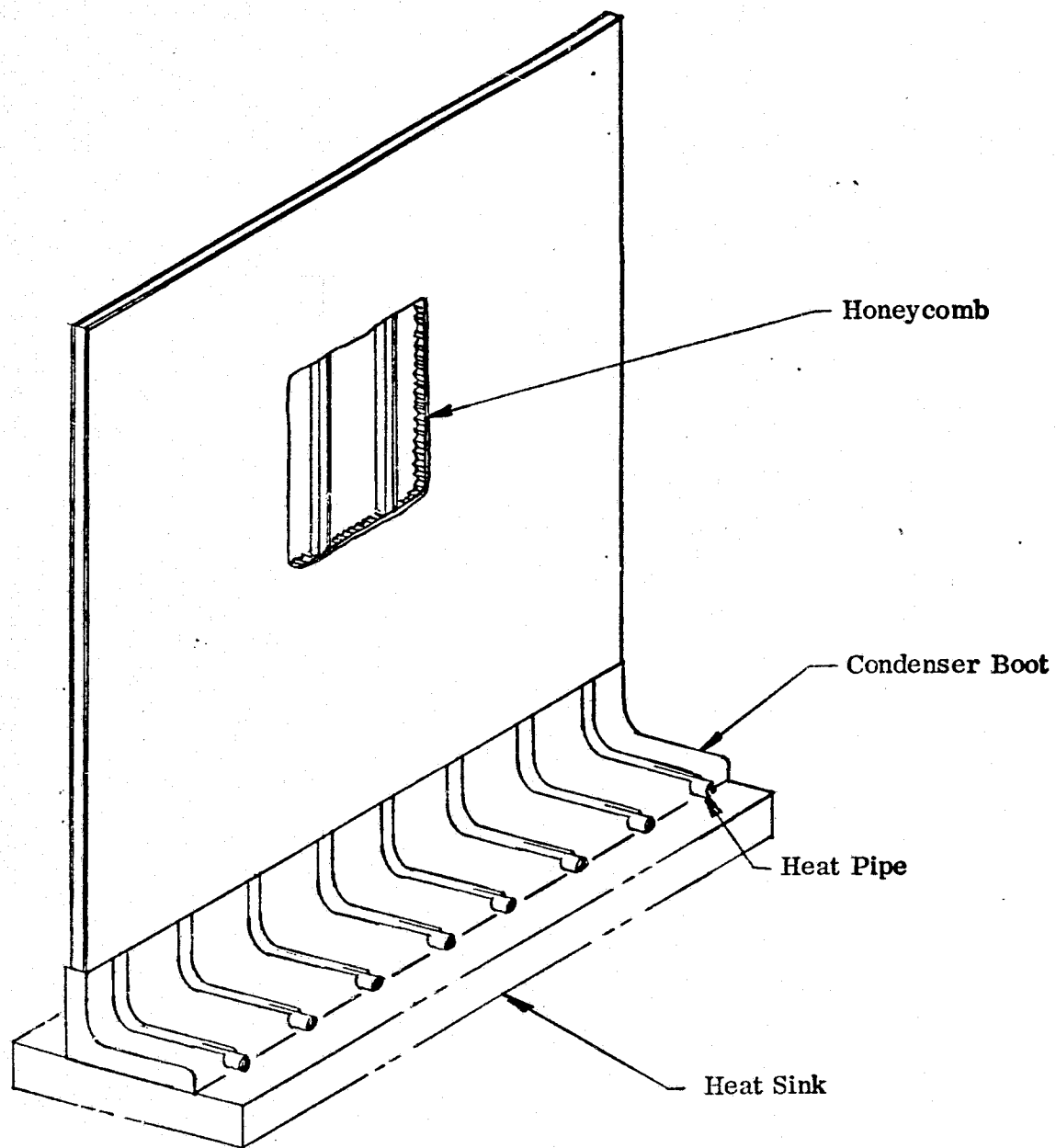


FIGURE 2.2-1. ISOPAC PANEL

FIGURE 2.2-2  
PERFORMANCE COMPARISON OF MAGNESIUM CELL  
SEPARATORS AND ISOPAC PANEL

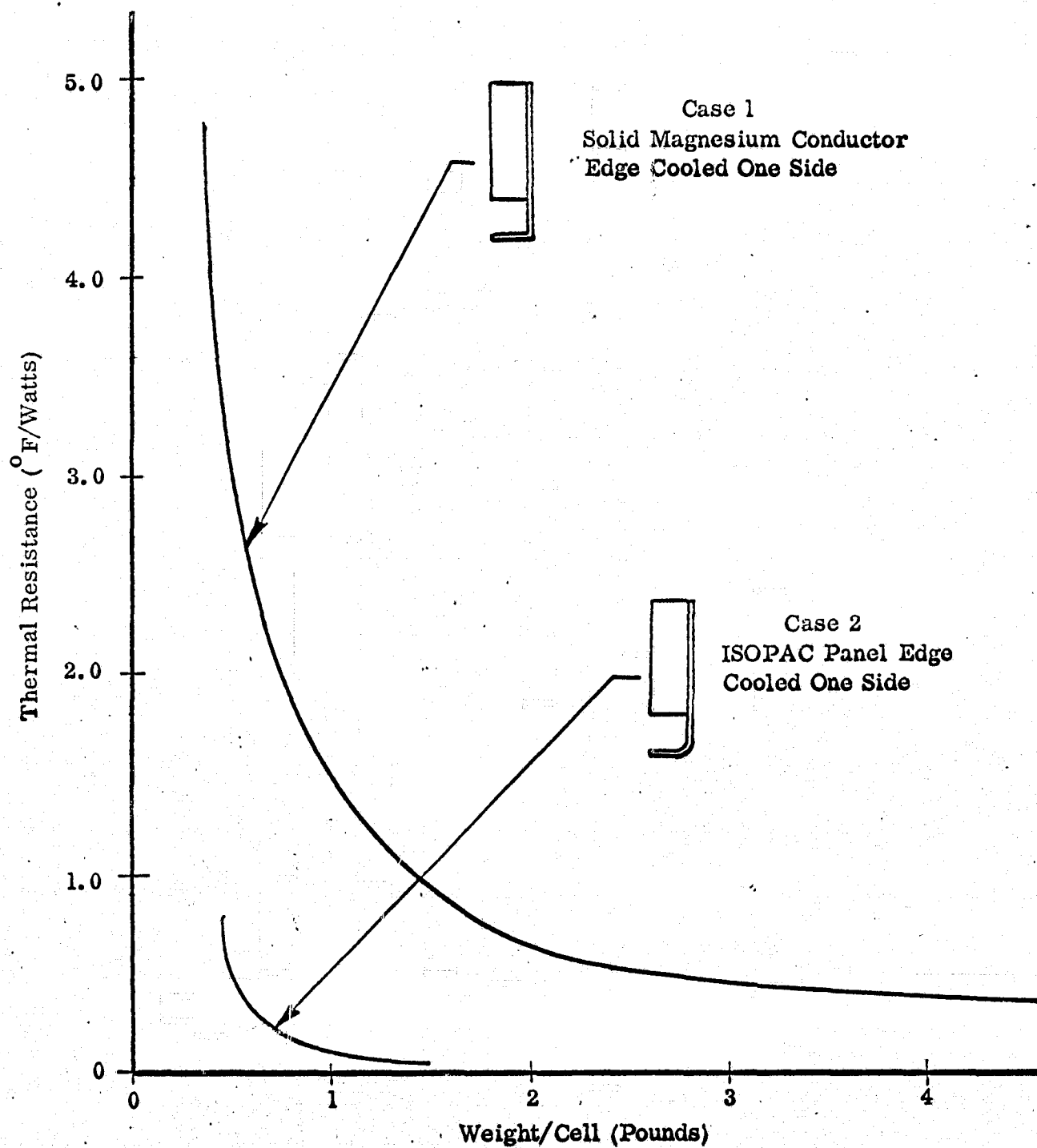


TABLE 2.2-1. DESIGN PARAMETERS OF ISOPAC PANEL

Number of Heat Pipes . . . . .	8
Heat Pipe Diameter . . . . .	3/16" (prior to machining)
Working Fluid . . . . .	Ammonia
Wick Structure . . . . .	6 layers of 200 mesh stainless steel screen inserted diametrically
Evaporator Length . . . . .	7.63"
Condenser Length . . . . .	1.50"
Overall Heat Pipe Length . . . . .	8.75"
Panel Geometry . . . . .	"L" Shaped (8.70" x 7.22" x 1.50")
Panel Construction . . . . .	1/8" Cell size aluminum honeycomb covered with 0.020 aluminum face sheets

TABLE 2.2-2. CALCULATED ISOPAC PERFORMANCE

<u>Type of Impedance</u>	<u>Type of Installation</u>	<u>°F/Watt</u>
Between surface of ISOPAC and condenser "boot"	Uniform heat input on one side (Case 1)	0.253
Between surface of ISOPAC and condenser "boot"	Uniform heat input on two sides (Case 2)	0.252
Between surface of ISOPAC and condenser "boot"	ISOPAC sandwiched between two uniform heat sources (Interface conductance = $250 \text{ Btu/Hr-Ft}^2\text{-}^\circ\text{F}$ ) (Case 3)	0.278
Between condenser "boot" and cold plate	ISOPAC mounted against ideal cold plate (Interface Conductance = $500 \text{ Btu/Hr-Ft}^2\text{-}^\circ\text{F}$ )	0.087
Overall Impedance	Case 1	0.340
Overall Impedance	Case 2	0.339
Overall Impedance	Case 3	0.365

reducing the total  $\Delta T$  between the cell and sink, the temperature gradient along the cell wall is eliminated by employing the ISOPAC panel. A breakdown of the thermal impedances of the ISOPAC panel is given in Table 2.2-2.

### 2.3 Variable Conductance Heat Pipes

The ISOPAC panel reduces the temperature difference between the cells and the heat sink; however, by itself, it does not control the temperature of the battery cells.

Fluctuations in battery temperature may be caused by two effects:

- Variations in the heat dissipated by the battery.
- Variations in the sink conditions; e. g., changes in the orientation of the spacecraft radiator or changes of the coolant temperature because of variations in the heat load on the system.

Performance and lifetime of the batteries could be improved if their temperature could be controlled within reasonable bands, independent of the heat dissipated and of sink conditions. It is for this reason that the Prototype Battery Heat Rejection System includes two (2) variable conductance (V/C) heat pipes as interfacing elements between the ISOPAC heat removal panels and the simulated spacecraft cold plate. The U-shaped V/C heat pipes are constructed of 1.0" diameter stainless steel tubing and are soldered at both ends to thermal interfacing plates (see Figure 1-2). The soldering of stainless steel tubing to aluminum interfacing plates was accomplished by having both plates coated in the bonding areas with a few mils of nickel plating. The evaporator section of the variable conductance heat pipe is soldered to an "intermediate" cold plate which, in turn, mechanically interfaces with the condenser "boot" of the ISOPAC panels. The condenser section of the V/C heat pipes is soldered to another plate which is directly interfaced with the simulated spacecraft cold plate. A two (2) heat pipe system was selected to

minimize the conductive path between the "boots" of the ISOPAC panels and the V/C heat pipe.

In Figure 2.3-1 the calculated thermal resistance between the "boots" of the ISOPAC panels and the working fluid of the V/C heat pipe is shown. It is seen that with two V/C heat pipes the resistance is substantially reduced. Little improvement is gained, however, by using more than two (2) V/C heat pipes. Furthermore, the "optimum" thickness of the intermediate cold plate is approximately 1/8 inch. Thicker cold plates would only increase the weight of the system but hardly improve the resistance.

The required operating temperature narrowed the choice of working fluids for the V/C heat pipes to methanol or ammonia. Methanol was chosen because of its smaller storage volume requirement for a given control sensitivity (Ref. 1). The storage volume is of the "cold type"; i. e., its temperature is coupled to that of the sink (cold plate).

The objective of using V/C heat pipes as interfacing elements between cell stack and cold plate is, of course, to minimize fluctuations of the cell temperature associated with changes in the heat load and/or sink temperature. It must be recognized, however, that the V/C heat pipes add additional thermal impedance to the system's resistance. If the sink temperature is well controlled, this additional impedance will actually cause larger excursions of the cell temperature than in the absence of V/C heat pipes.

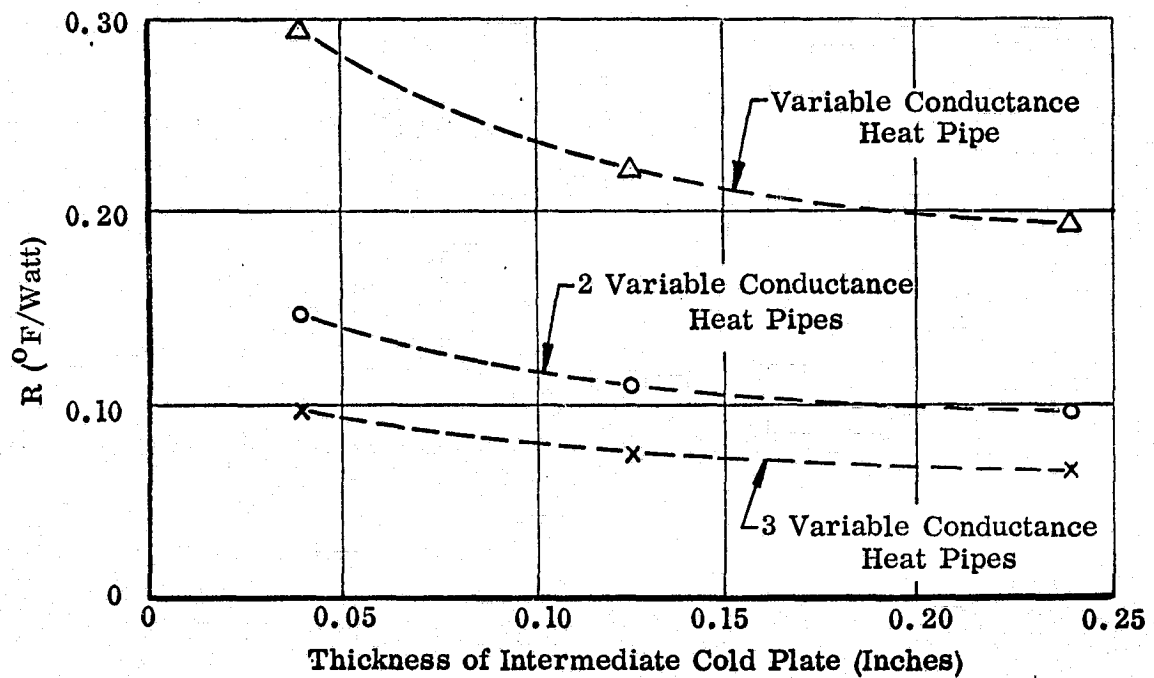
When the cell stack is heat sunk directly to the cold plate the cell temperature ( $T_c$ ) is related to the heat rate ( $\dot{Q}$ ) and the sink temperature ( $T_o$ ) through

$$T_c = R_c \dot{Q} + T_o \quad (1)$$

---

Ref. 1: Bienert, W., Brennan, P. J., and Kirkpatrick, J. P., "Feedback Controlled Variable Conductance Heat Pipes," AIAA Paper No. 71-421, 6th Thermophysics Conference, Tullahoma, Tennessee, April 1971

FIGURE 2.3-1  
CALCULATED RESISTANCE BETWEEN ISOPAC BOOTS  
& VAPOR OF VARIABLE CONDUCTANCE HEAT PIPE



where  $R_c$  is the thermal resistance of the cell stack. In case of a constant sink temperature the variations of the cell temperature become

$$\Delta T_c = R_c \Delta \dot{Q} \quad (2)$$

According to Table 2.2-2 the resistance between cells and cold plate was calculated as

$$R_c = \frac{1}{6} (.278 + .087) = .061^\circ\text{F/watt}$$

Hence, if the heat dissipated varies between zero and 125 watts the corresponding fluctuation of the cell temperature will be  $125 \times .061 = 7.6^\circ\text{F}$ .

When the cell stack is heat sunk through V/C heat pipes their own evaporator and condenser resistances add to the total impedance of the system. The cell temperature is then given by

$$T_c = R_c \dot{Q} + R_{\text{evap}} \dot{Q} + R_{\text{cond}} \dot{Q} + T_o \quad (3)$$

where  $R_{\text{evap}}$  and  $R_{\text{cond}}$  are the internal resistances of the V/C heat pipes. The condenser resistance is variable and self-adjusting such that the vapor temperature of the V/C heat pipe is maintained nearly constant. In case of a constant sink temperature the variations of the cell temperature become

$$\Delta T_c = (R_c + R_{\text{evap}}) \Delta \dot{Q} + \Delta(R_{\text{cond}} \dot{Q}) \quad (4)$$

For an ideal V/C heat pipe the second term on the right-hand side of (4) approaches zero (Ref. 2) and the variation of the cell temperature is

$$\Delta T_c = (R_c + R_{\text{evap}}) \Delta \dot{Q} \quad (5)$$

Using the same values for the stack resistance as above ( $1/6 \times .278^\circ\text{F/watt}$ ) and an evaporator resistance of the V/C heat pipe of  $0.110^\circ\text{F/watt}$  (based on Figure 2.3-1 for two (2) V/C heat pipes and a  $1/8$ " thick cold plate) the corresponding temperature fluctuation of

---

Ref. 2: Bienert, W., "Heat Pipes for Temperature Control," Intersociety Energy Conv. Conference, September 1969, pp. 1033-1041



the cells becomes

$$\Delta T_c = \left(\frac{1}{6} \times .278 + 0.110\right) \times 125 = 19.6^\circ \text{F}$$

This example demonstrates that a variable conductance heat pipe is undesirable if the sink temperature is constant. If however the sink temperature fluctuates the V/C heat pipe will attenuate these fluctuations. This is accomplished through a compensating change in the condenser resistance. In the special case where the heat rate is constant ( $\dot{Q} = 0$ ) the fluctuations of the cell temperature are related to changes in the sink temperature through

$$\Delta T_c = \dot{Q} \Delta R_{\text{cond}} + \Delta T_o \quad (6)$$

For an ideal V/C heat pipe, the adjustment of condenser resistance completely compensates for changes of the sink temperature and the cell temperature remains constant.

The ideal V/C heat pipe requires an infinite gas storage volume. With gas storage volumes of finite and practical size, much larger variations of the cell temperature must be expected. An approach for attaining nearly absolute control of the cell temperature is a feedback controlled V/C heat pipe. In such a system the temperature of a "wet" storage volume is controlled by an auxiliary heater which, in turn, is regulated through a feedback loop which monitors the cell temperature automatically. Since this feature was beyond the scope of the contract, only a manual control for a heater of the gas storage volume was provided as an option for testing.

The analysis conducted on the V/C heat pipes resulted in the design parameters indicated in Table 2.3-1.

The design of wick and gas storage volume of the V/C heat pipes is shown in Figure 2.3-2.

FIGURE 2.3-2

DESIGN OF WICK AND GAS STORAGE VOLUME  
OF VARIABLE CONDUCTANCE HEAT PIPES

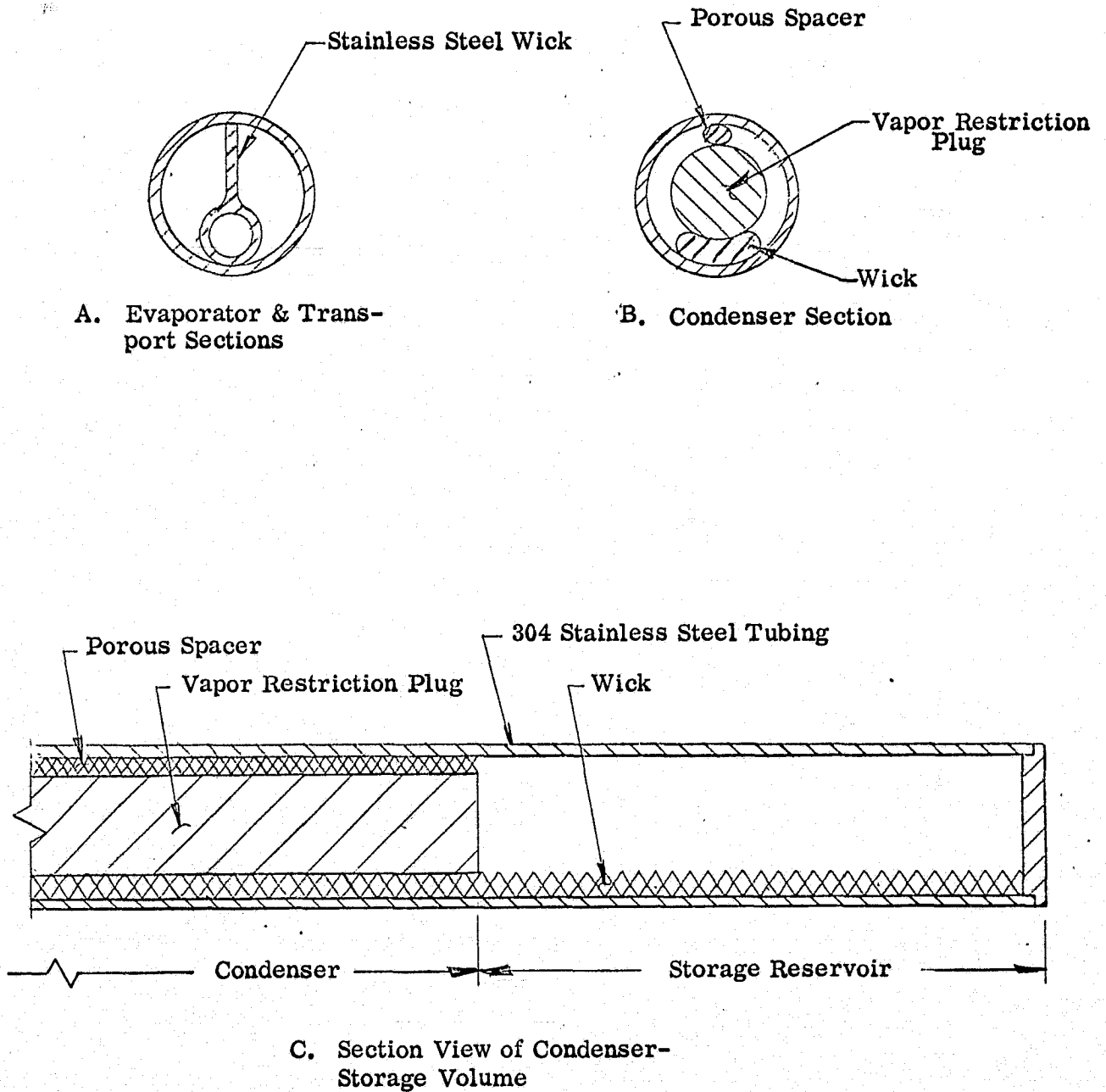


TABLE 2.3-1

DESIGN PARAMETERS OF VARIABLE CONDUCTANCE HEAT PIPES

Length of Heat Pipes . . . . .	30.0 inches
Outer Diameter . . . . .	1.0 inch
Working Fluid . . . . .	Methanol
Noncondensing Gas . . . . .	Argon
Geometry . . . . .	U-Shaped
Evaporator Length . . . . .	10.0 inches
Condenser Length . . . . .	10.0 inches
Gas Storage Volume . . . . .	2.4 inches <sup>3</sup>
Ratio of Gas Storage Volume to Condenser Volume . . .	1.0
Required Heat Transport Capability . . . . .	62.5 W (min)

## 2.4 Pressure Retention Plates

The heat removal capability of the ISOPAC panels is directly related to the degree of interface contact existing between cells and ISOPACS. Because of the variation in internal cell pressures during the typical charge-discharge cycles of the battery, a preload/clamping mechanism was designed. Internal cell pressures of 40 psia are not uncommon during a charge-discharge cycle. The preload/clamping mechanism was therefore designed to accommodate this worst case internal pressure.

The preload/clamping mechanism consists of two (2) pressure retention plates and eight (8) threaded tie-rods. The pressure retention plates were fabricated from 6061 aluminum plate and were sized to be capable of limiting the midspan deflection of the cell cases to less than 0.005" during the 40 psi internal pressure condition. With the ISOPAC panels placed between the cells, the pressure retention plates are located at the ends of the battery stack. The eight (8) stainless steel 1/4-28 threaded tie-rods are tightened uniformly to a torque of 25-30 inch-pounds. This method of preloading the battery stack not only restrains the cells from dimensional excursions but actually benefits the thermal operation of the entire Prototype Battery Heat Rejection System. The preload technique improves the interface contact between the ISOPAC and the adjoining cell thus enhancing the removal of the heat to the cold plate or V/C heat pipes.

## 2.5 Simulated Spacecraft Cold Plate

To demonstrate the capability of the Spacecraft Battery Heat Rejection System it was necessary to provide a simulated spacecraft cold plate. The cold plate consists of an aluminum plate with a coolant channel brazed to the underside which is in turn connected to a liquid coolant circulation unit via flexible lines. The Prototype Battery Heat Rejection System is mechanically interfaced with the simulated spacecraft cold

plate to dump the heat removed from the battery stack.

The liquid coolant circulation unit selected for this program was supplied by Forma-Scientific. The unit circulates a 50% solution of ethylene glycol and water through the aluminum cold plate to maintain the cold plate at a uniform temperature. The coolant circulation unit is capable of controlling the temperature of the coolant in the  $-4^{\circ}\text{F}$  to  $+158^{\circ}\text{F}$  range with an accuracy of  $\pm 0.04^{\circ}\text{F}$ . The unit while interfaced with the heat rejection system is capable of accommodating the maximum heat load of 125 watts over the entire temperature range while limiting the bulk coolant temperature increase to less than  $5^{\circ}\text{F}$ .

### 3. THERMAL PERFORMANCE TESTS

Performance testing of the Spacecraft Battery Heat Rejection System consisted of a thermal test to demonstrate the compliance of the system to the heat removal requirements. The performance tests of the system were conducted in an orderly component-by-component buildup fashion:

- ⊙ Individual ISOPAC Panel and the Simulated Cold Plate
- ⊙ ISOPAC Panels integrated with the Battery Thermal Mock-Ups and sinked by the Simulated Cold Plate
- ⊙ Total Spacecraft Battery Heat Rejection System without the Auxiliary Power to the Storage Volumes
- ⊙ Total Spacecraft Battery Heat Rejection System with the Auxiliary Power to the Storage Volumes

#### 3.1 ISOPAC Panel and Simulated Cold Plate

The first component test conducted consisted of one ISOPAC panel interfaced directly with the simulated spacecraft cold plate (chill plate). Figure 3.1-1 shows the electrical heaters and thermocouple locations on the ISOPAC panel. The purpose of this initial test was to establish the ISOPAC thermal resistance and the interface resistance inherent to the system.

Strip heaters were bonded to one side of the panel and covered the entire surface with exception of narrow gaps between the heaters where the thermocouples were located. Heat was applied fairly uniformly over the entire evaporator section of the ISOPAC panel. The ISOPAC panel was tested in the level orientation at two heater input powers (12.1 and

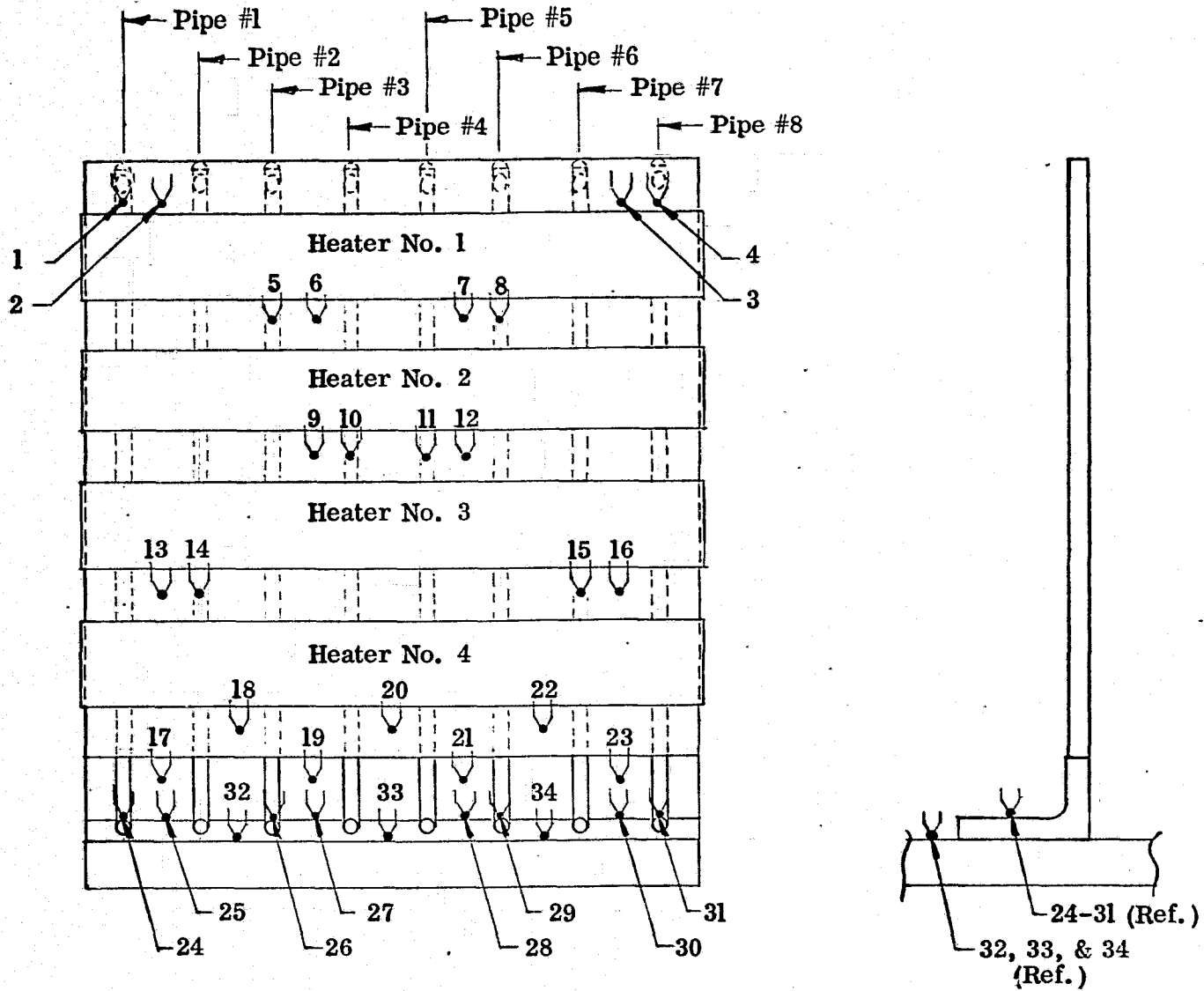


FIGURE 3.1-1

TEST OF INDIVIDUAL ISOPAC PANEL - INSTRUMENTATION DIAGRAM

25.5 watts) and at several liquid coolant temperatures ( $-12^{\circ}\text{F}$  up to  $+68^{\circ}\text{F}$ ). The entire setup was wrapped with fiberglass insulation to minimize the effects of variations in ambient conditions. By placing all the heaters on one face of the ISOPAC panel, a worst case condition is simulated. Under normal operating conditions heat is applied uniformly on both sides of the panel; therefore, the test runs with 25.5 watts input power represent a worst case situation.

A summary of the data taken during this initial test is tabulated in Table 3.1-1. Test data indicates that the thermal resistances for the ISOPAC panel and the interface contact remain essentially constant for the two heater input powers over the range of liquid coolant temperatures. An average ISOPAC thermal resistance of  $0.385^{\circ}\text{F/Watt}$  between the heat input area and the cold plate was determined. The average interface contact resistance (between the ISOPAC condenser section and the cold plate) was measured to be  $0.075^{\circ}\text{F/Watt}$ . Slight variations in thermal resistances for different liquid coolant temperatures represent the effect of variations in ambient conditions. The measured contact resistance between the precision machined surfaces (flat within .002) of the ISOPAC boot and the cold plate (chill plate) yields an effective film coefficient ( $h_{\text{eff}}$ ) of  $555 \text{ Btu/Hr-Ft}^2\text{-}^{\circ}\text{F}$ . A comparison of the measured thermal impedances with the analytical prediction is given in Table 3.1-2.

TABLE 3.1-2  
COMPARISON OF MEASURED AND PREDICTED  
THERMAL IMPEDANCES OF ISOPAC PANEL

Type of Impedance	Predicted	Measured
Between surface of ISOPAC and condenser boot	$.253^{\circ}\text{F/Watt}$	$.306^{\circ}\text{F/Watt}$
Interface between condenser boot and cold plate	$.087^{\circ}\text{F/Watt}$	$.079^{\circ}\text{F/Watt}$



TABLE 3.1-1

ISOPAC PERFORMANCE TEST RESULTS

(Individual ISOPAC Heated Uniformly on One Side,  
Mounted on "Ideal" Cold Plate)

Heater Input Power (Watts)	Coolant Bath Temperature (°F)	Thermal Resistances (°F/Watt)	
		ISOPAC Panel*	Interface Contact**
14.4	-12	0.488	0.083
25.5		0.341	0.102
12.1	+14	0.355	0.116
25.5		0.255	0.063
12.1	+32	0.306	0.116
25.5		0.271	0.067
12.1	+50	0.289	0.058
25.5		0.267	0.074
12.1	+68	0.264	0.041
25.5		0.219	0.067
	Average	0.306	0.079

\*Thermal resistance between surface of ISOPAC and condenser "boot".

\*\*Interface resistance between condenser "boot" and cold plate.

The measured impedance of the ISOPAC panel is within 20% of the predicted value. This small discrepancy can be related to the film coefficients at the evaporators and condensers of the ammonia heat pipes which are difficult to evaluate. The measured interface resistance between ISOPAC's and cold plate corresponds to a film coefficient of 555 Btu/Hr-Ft<sup>2</sup>-°F which is close to the assumed value of 500 Btu/Hr-Ft<sup>2</sup>-°F.

In comparison to a purely conductive spacer the ISOPAC panel also reduces temperature gradients along the battery cells. In Figure 3.1-2 the measured temperature gradient along the ISOPAC is shown for a typical heat input of 25 watts. Superimposed on this figure is the calculated temperature distribution for an aluminum spacer of equal weight and geometry.

The preceding results indicate a good correlation between the predicted performance of the ISOPAC panel and actual test results. Based on comparable installations, the ISOPAC not only alleviates temperature gradients within the cell but also reduces greatly the thermal impedance between cells and cold plate.

### 3.2 ISOPAC Panel, Battery Thermal Mock-Up, and Simulated Cold Plate

The next step in the testing process was to sandwich six (6) ISOPAC panels between the cells of the thermal mock-up. Using the pressure retention plates to preload the battery stack, the assembly was then directly interfaced with the simulated cold plate (chill plate). The purpose of this test was to evaluate the heat removal capability of the ISOPAC panels and to evaluate the effect of various cell internal pressures on their performance without the added complexity of the variable conductance heat pipes. All tests were conducted with a coolant temperature of 32°F while the individual cell pressures were varied from 0 to 40 psia. The measured overall thermal resistance of the simulated battery is shown in Figure 3.2-1 as a function of cell pressure. This resistance is defined as the

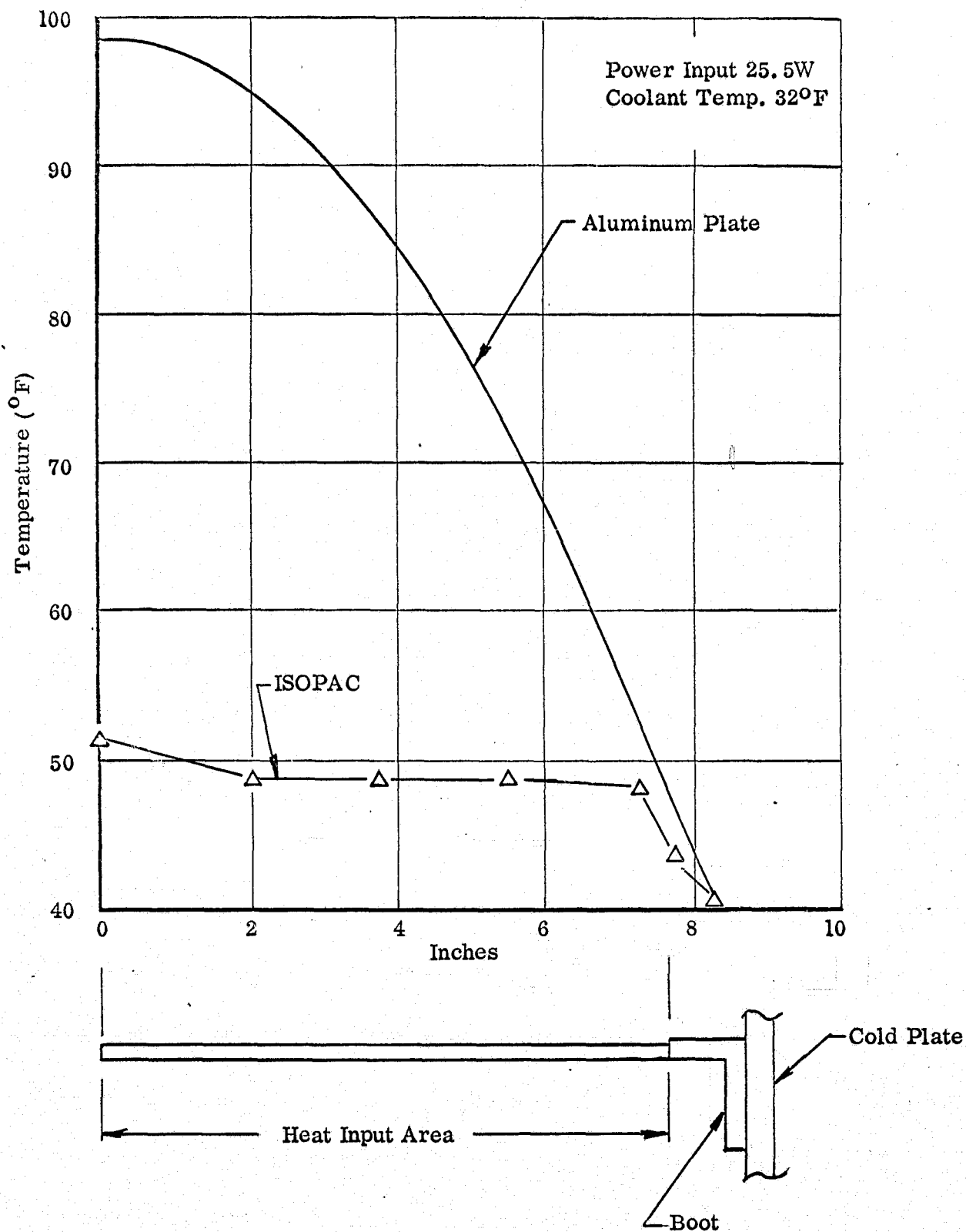


FIGURE 3.1-2  
TEMPERATURE GRADIENT WITHIN ISOPAC AND  
EQUIVALENT ALUMINUM SPACER OF EQUAL WEIGHT

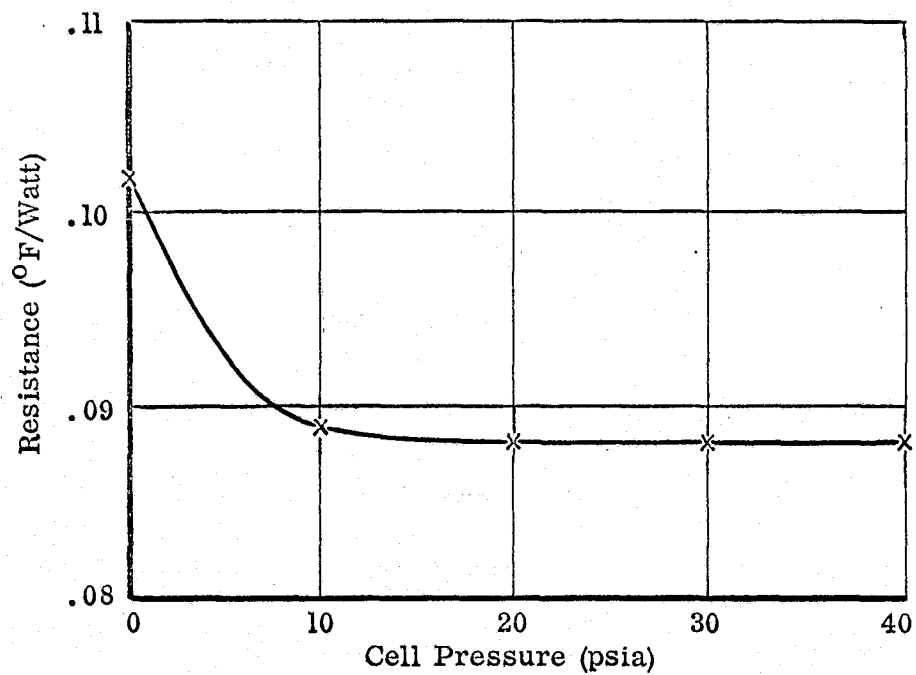


FIGURE 3.2-1

THERMAL RESISTANCE BETWEEN CELLS & COLD PLATE  
AS A FUNCTION OF CELL PRESSURE  
(ISOPAC Panel Used As Spacers Between Cells)

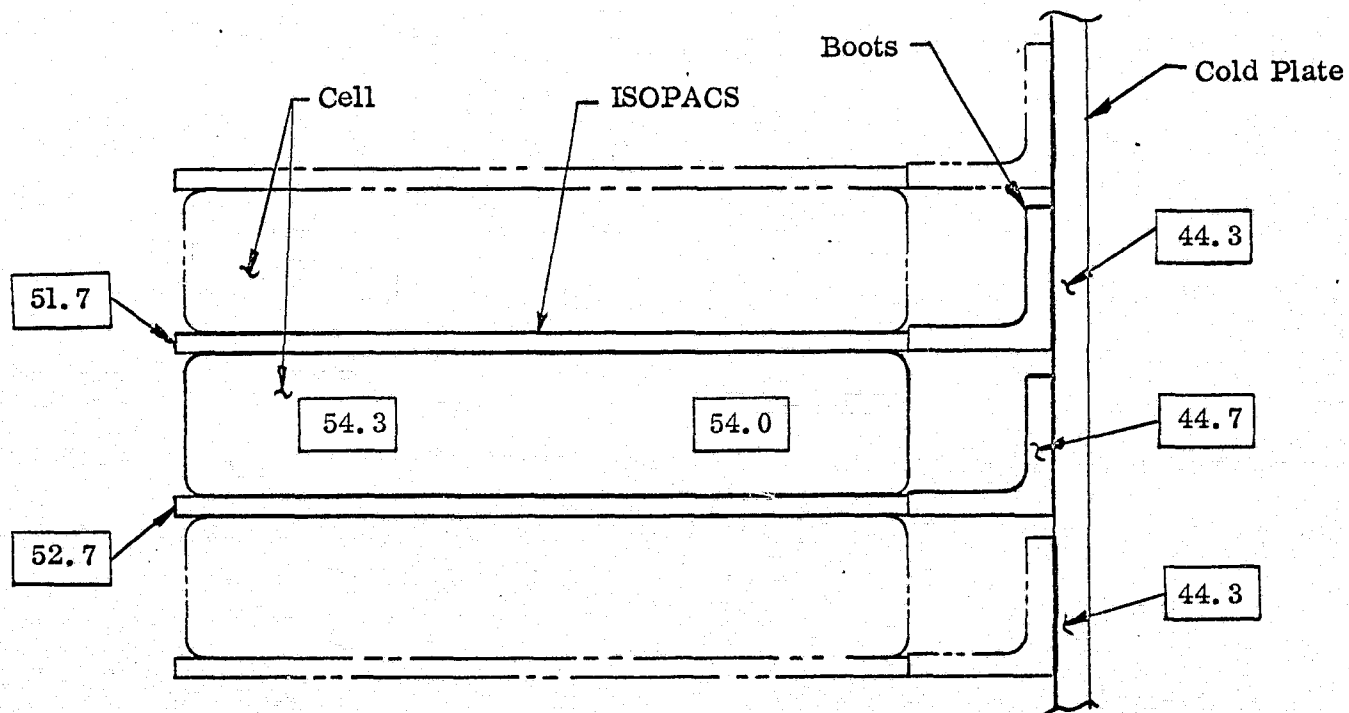


FIGURE 3.2.2

TYPICAL TEMPERATURE DISTRIBUTION (°F)  
WITHIN CELL STACK WITH ISOPAC SPACERS

temperature difference between the interior of the cells and the cold plate for a unit heat input. It includes the interface resistance between cells and ISOPAC's and between ISOPAC's and cold plate. As anticipated, the overall resistance decreases with increasing cell pressure, at least up to a certain threshold pressure of approximately 20 psia; beyond that, the resistance is constant. The improvement with increased pressure is, of course, due to better contact resistance between cell and ISOPAC at higher pressures.

A typical temperature distribution for a section of the battery is shown in Figure 3.2-2. As pointed out earlier, the ISOPAC not only reduces the overall temperature difference between cells and sink but also eliminates gradients. The measured thermal resistance between cells and sink can be compared with the performance of an individual ISOPAC panel. Since there were six (6) panels in the pack the equivalent resistance per panel is equal to  $6 \times 0.082 = 0.490^{\circ}\text{F/Watt}$ . Considering the fact that this resistance includes the temperature gradient within the cells as well as all interface resistances it compares well with the value of  $0.306 + 0.079 = 0.385^{\circ}\text{F/Watt}$  for the individual panel.

### 3.3 Testing of Complete Prototype of Battery Heat Pipe Heat Rejection System

The final tests were conducted with the completely assembled prototype system including the variable conductance heat pipes. A performance test schematic is shown in Figure 3.3-1. The pressure within the cells was maintained constant at 40 psia. The majority of the tests were conducted with the gas storage reservoir coupled to the sink temperature; i. e., without any auxiliary heat input which is representative of a "cold" storage reservoir. Because of the long time period required for the system to reach thermal equilibrium ( $\sim 8$  hours) the number of test conditions was limited to the following matrix (Table 3.3-1):

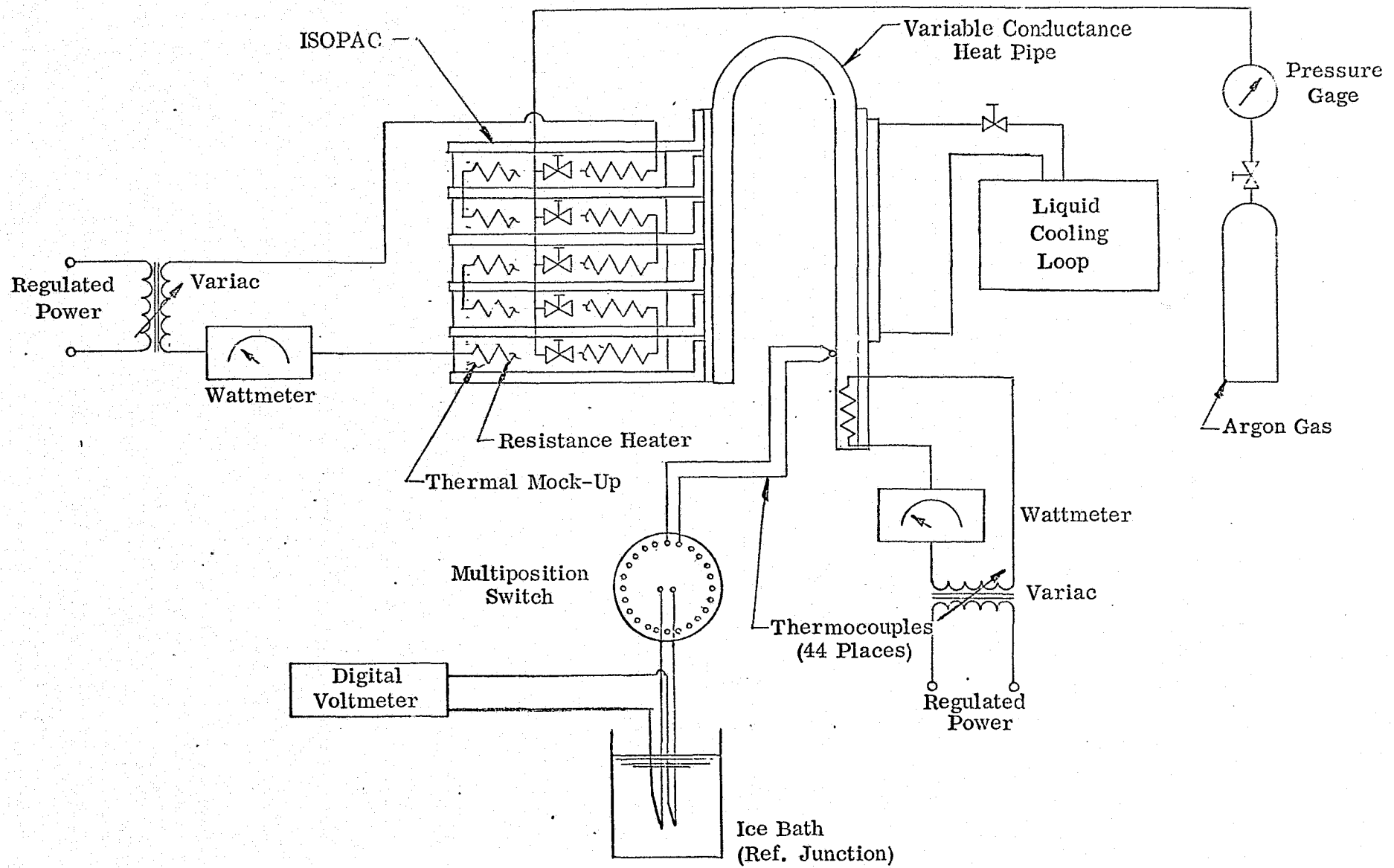


FIGURE 3.3-1  
PERFORMANCE TEST SCHEMATIC

TABLE 3.3-1. TEST CONDITIONS FOR COMPLETE PROTOTYPE BATTERY HEAT REJECTION SYSTEM

Gas Storage Reservoir	Sink Temperature (°F)	Heat Dissipated by Cell Stack (Watts)
Coupled to Sink ("Cold")	-4	0, 50, 100, 125
	+32	0, 75, 100, 125
	+68	0, 75, 100
Heated to Vapor Temperature (15 Watts Input)	-4	100
	+32	100

For the two low sink temperatures (-4 and +32°F) the maximum heat dissipated by the cell stack was 125 Watts (25 Watts/cell) at the high sink temperature of 68°F the heat load was limited to 100 W in order to avoid excess cell temperatures. During testing with a heated gas storage reservoir the heat load to the cell stack was held constant at 100 Watts. The objective was to obtain optimum control of the cell temperature for a wide variation of sink temperatures.

The actual test results for each of the above test conditions are given in Appendix A along with a chart showing the location of all 44 thermocouples used for mapping the temperature distribution. In Appendix B the test results are summarized in terms of average temperatures of cells, ISOPAC's, variable conductance heat pipes, cold plates, etc.

A performance summary of the Prototype Heat Pipe Battery Heat Rejection System is given in Figures 3.3-2 through 3.3-6. In Figure 3.3-2 the average measured cell temperature is plotted as a function of sink temperature for two modes of heat generation; i.e.,  $\dot{Q} = 0$ , and  $\dot{Q} = 100$  Watts. Also shown in that figure is the predicted variation of cell temperatures without the use of variable conductance heat pipes. The prediction was based on the measured thermal resistance of the cell stack when interfaced

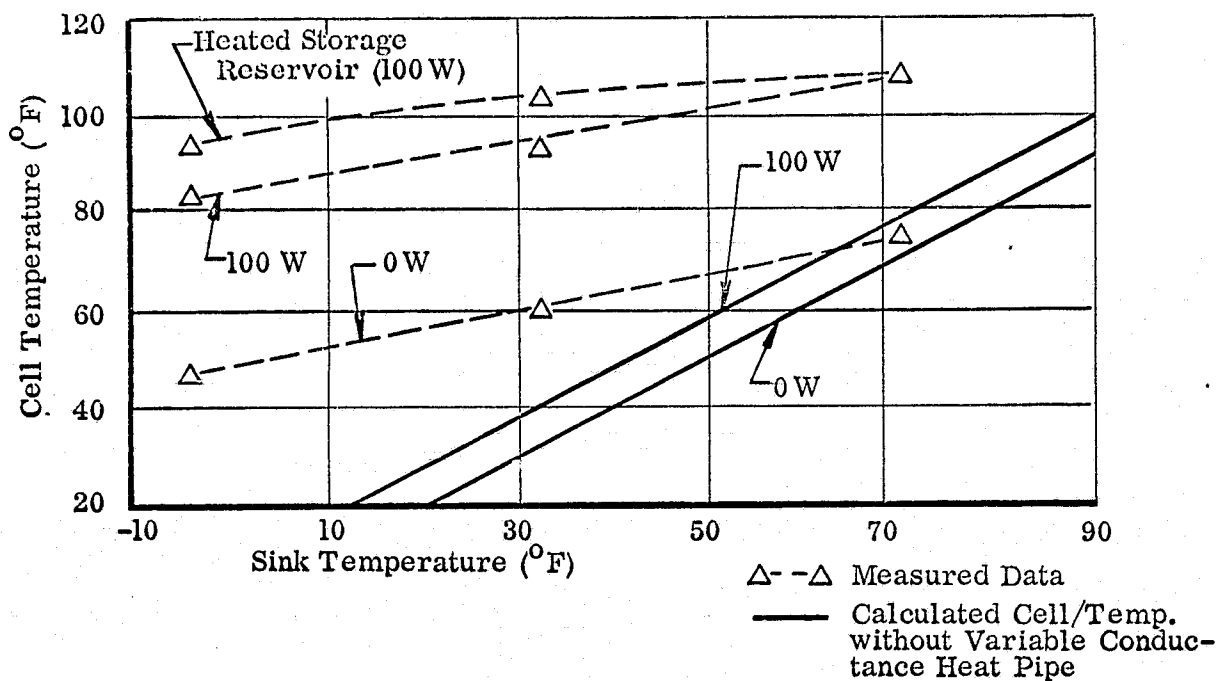


FIGURE 3.3-2

MEASURED CELL TEMPERATURE AS A FUNCTION OF SINK TEMPERATURE  
(PARAMETER: HEAT LOAD)

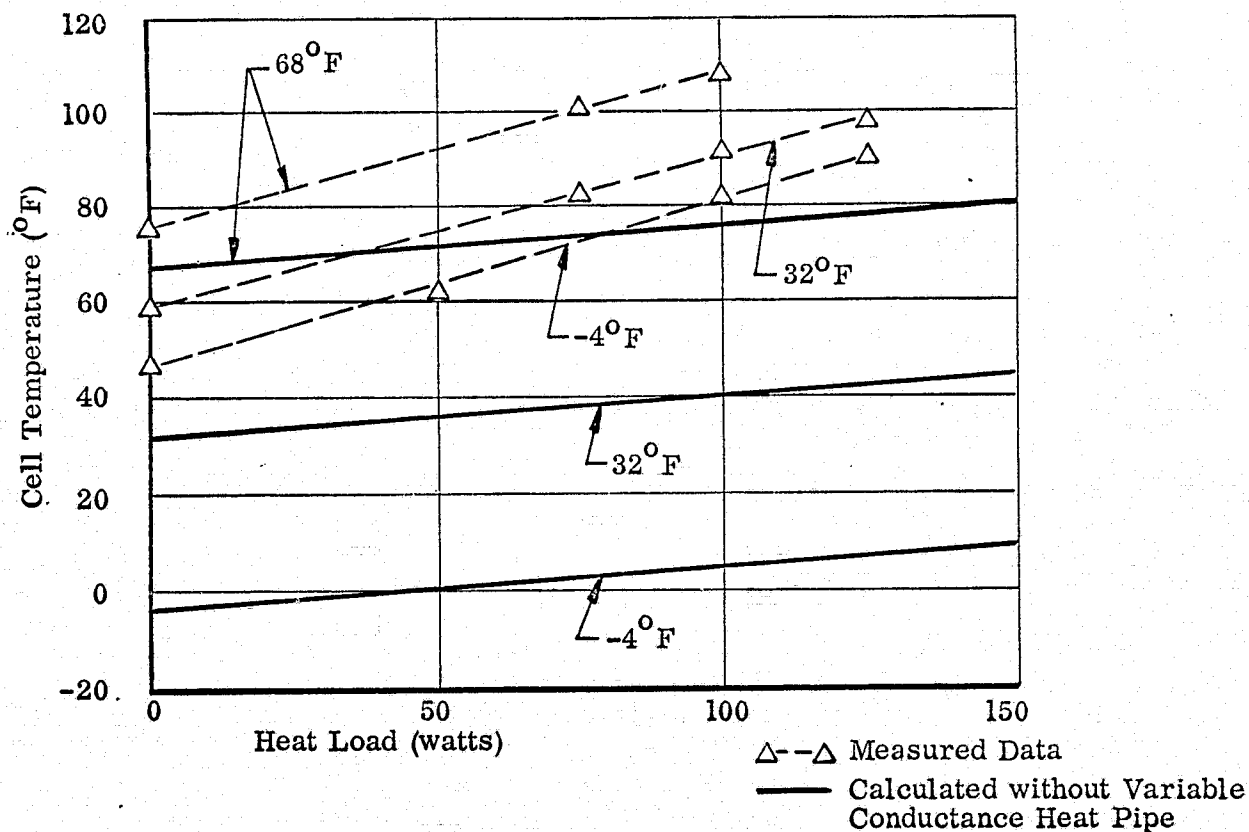


FIGURE 3.3-3

MEASURED CELL TEMPERATURE AS A FUNCTION OF HEAT DISSIPATED  
(PARAMETER: SINK TEMPERATURE)



directly with an ideal cold plate (see Section 3.2). It can be seen from this figure that the effect of sink temperature variation is greatly reduced by the variable conductance heat pipes. The additional resistance which is introduced by the variable conductance heat pipes causes the cells, of course, to operate at a higher temperature for a given sink than would be experienced with direct coupling. Figure 3.3-3 gives the measured cell temperatures as a function of the heat dissipated by the cells with the sink temperature as a parameter. The maximum system temperature difference between cells and sink is plotted in Figure 3.3-4. This temperature difference increases with decreasing sink temperature which shows the stabilizing effect of the variable conductance heat pipes.

A quantitative evaluation of the control capability of the prototype system is given in Figures 3.3-5 and 3.3-6. Both figures give the measured resistance between cells and sink. In Figure 3.3-5 the overall resistance is plotted as a function of sink temperature for a constant heat input. Varying the sink temperature from  $-4^{\circ}\text{F}$  to  $+68^{\circ}\text{F}$  changes the resistance by approximately a factor of two (2). This variation of the overall resistance results in the reduced temperature sensitivity of the cell stack as shown in Figures 3.3-2 and 3.3-3.

The variable conductance heat pipes also reduce temperature fluctuations resulting from variations in the heat dissipated by the cells. This effect is shown in Figure 3.3-6, in which the overall thermal resistance is plotted as a function of heat input for one particular sink temperature ( $-4^{\circ}\text{F}$ ). The decrease of the overall resistance with increasing heat load again reflects the stabilizing effect of the variable conductance heat pipes.

Because of time limitations, only two (2) tests were conducted with a heated gas storage reservoir. As indicated in Table 3.3-1, during these tests the heat dissipated

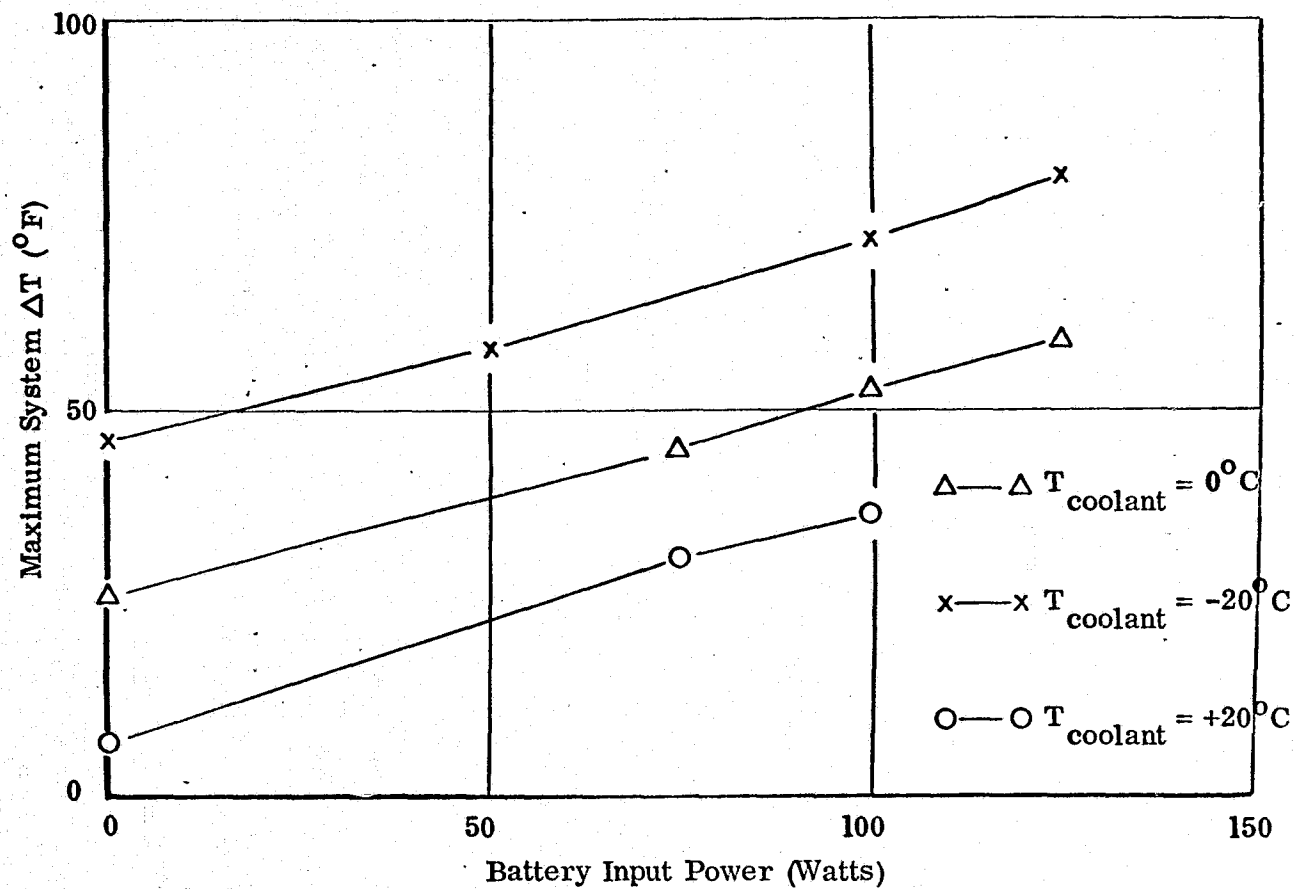


FIGURE 3.3-4  
MAXIMUM HEAT REJECTION SYSTEM TEMPERATURE  
DROP AS A FUNCTION OF BATTERY INPUT POWER

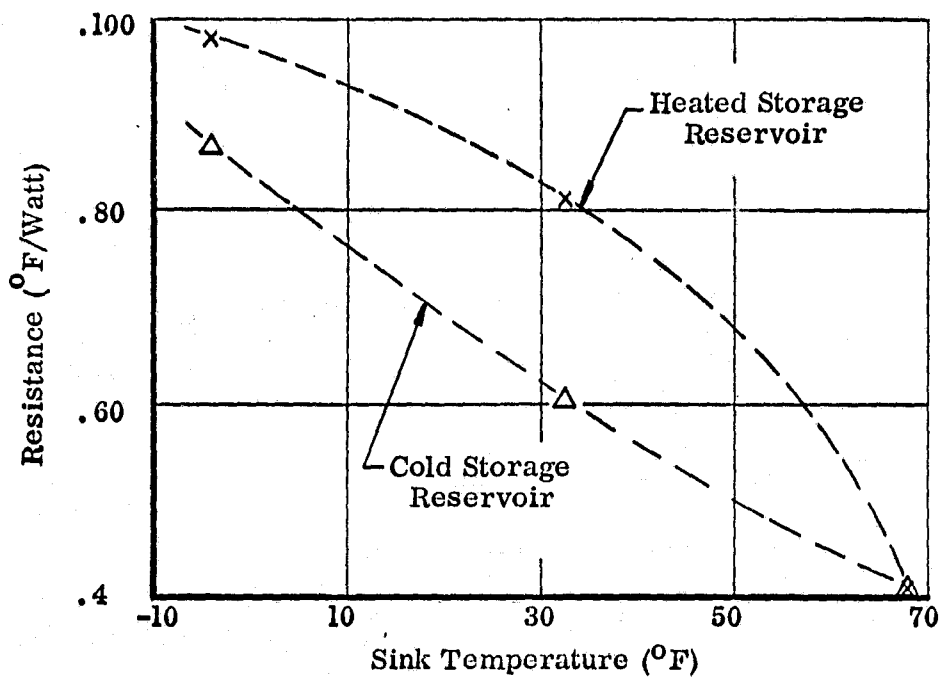


FIGURE 3.3-5  
SYSTEM RESISTANCE AS A FUNCTION OF SINK TEMPERATURE  
(Heat Load Constant at 100 Watts)

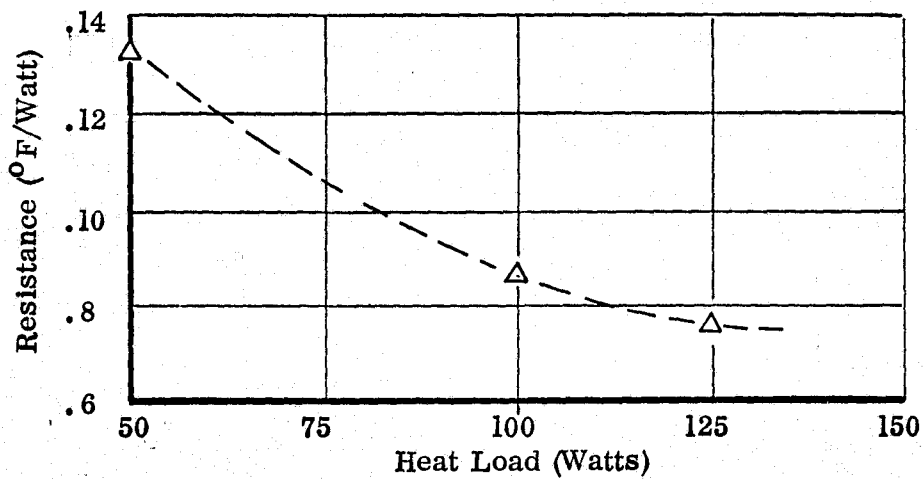


FIGURE 3.3-6  
SYSTEM RESISTANCE AS A FUNCTION OF HEAT LOAD  
(Sink Temperature at  $-4^{\circ}\text{F}$ )

by the cells was held constant at 100 watts and the sink temperature was varied between  $-4$  and  $+32^{\circ}\text{F}$ . The input into the storage reservoir was limited by the condition that maximum control is afforded when all noncondensable gas is driven out of the storage reservoir. This condition is reached when the temperature of the storage reservoir equals that of the vapor of the variable conductance heat pipes. The vapor pressure of the working fluid in the storage reservoir is then equal to that in the active portion of the heat pipes and, consequently, all of the noncondensable gas is located in and blocking the condenser, thus resulting in a maximum system resistance. The effect of heating the gas storage reservoir is shown in Figure 3.3-2. While it was not possible to maintain the cell temperature completely constant, the variations were reduced to  $12^{\circ}\text{F}$ . Considering that the sink temperature varied at the same time by  $72^{\circ}\text{F}$  the control capability of this system is well demonstrated. Independent experiments with feedback controlled variable conductance heat pipes have shown that absolute control of the battery temperature is feasible using the approach of heated gas storage reservoirs. The prototype battery heat rejection system was not designed for feedback control of the cell temperature. However, minor modifications of the gas storage volume along with an automatic feedback system could yield a battery heat rejection system which would provide absolute control of the battery temperature during all phases of the charge-discharge cycle and for all practical sink conditions.

## APPENDIX A

### **TEST DATA AND INSTRUMENTATION**

# PITCH PERFORMANCE TESTS

## (SHEET #1)

PERFORMANCE TEST RUNS													
	# 1		# 2		# 3		# 4		# 5		# 6		
DATE	4-1-71		4-8-71		4-9-71		4-9-71		4-7-71		4-7-71		COMMENTS
TIME	8:50		13:00		8:35		11:45		8:35		16:40		
POWER	0W		75W		100W		125W		0W		50W		
BATH TEMP	32°F		32°F		32°F		32°F		-40°F		-40°F		
BATTERY PRESSURE	40#/IN <sup>2</sup>		40#/IN <sup>2</sup>		40#/IN <sup>2</sup>		40#/IN <sup>2</sup>		40#/IN <sup>2</sup>		40#/IN <sup>2</sup>		
T/C #1	.78	59.7	1.39	81	1.66	90.3	1.80	95	.42	47	.81	60.7	BATTERY #1
" 2	.77	59.3	1.39	81	1.66	90.3	1.80	95	.42	47	.81	60.7	
" 3	.77	59.3	1.43	82.3	1.72	92.3	1.88	98	.42	47	.85	62.3	BATTERY #2
" 4	.77	59.3	1.43	82.3	1.72	92.3	1.88	98	.42	47	.84	62	
" 5	.77	59.3	1.46	83.3	1.75	93.3	1.95	100.3	.42	47	.88	63.3	BATTERY #3
" 6	.77	59.3	1.46	83.3	1.76	93.7	1.95	100.3	.42	47	.88	63.3	
" 7	.77	59.3	1.46	83.3	1.76	93.7	1.93	99.7	.42	47	.88	63.3	BATTERY #4
" 8	.77	59.3	1.47	83.7	1.76	93.7	1.93	99.7	.44	47.7	.89	63.7	
" 9	.78	59.7	1.45	83	1.73	92.7	1.92	99.3	.44	47.7	.88	63.3	BATTERY #5
" 10	.78	59.7	1.45	83	1.72	92.3	1.92	99.3	.44	47.7	.88	63.3	
" 11	.78	59.7	1.33	79	1.57	87.3	1.68	91	.44	47.7	.77	59.3	ISOPAC #1
" 12	.76	59	1.26	76.3	1.47	83.7	1.57	87.3	.41	46.7	.71	57.3	
" 13	.78	59.7	1.38	80.7	1.63	89.3	1.78	94.3	.43	47.3	.81	60.7	ISOPAC #2
" 14	.76	59	1.29	77.3	1.53	85.7	1.64	89.7	.40	46.3	.73	58	
" 15	.78	59.7	1.41	81.7	1.67	90.7	1.85	97	.44	47.7	.84	62	ISOPAC #3
" 16	.76	59	1.31	78.3	1.55	86.7	1.69	91.3	.41	46.7	.75	58.7	
" 17	.78	59.7	1.43	82.3	1.71	92	1.88	98	.44	47.7	.86	62.7	ISOPAC #4
" 18	.76	59	1.32	78.7	1.56	87	1.72	92.3	.40	46.3	.77	59.3	
" 19	.79	60	1.42	82	1.68	91	1.86	97.3	.45	48	.86	62.7	ISOPAC #5
" 20	.76	59	1.32	78.7	1.56	87	1.71	92	.41	46.7	.77	59.3	
" 21	.80	60.3	1.37	80.3	1.62	89	1.78	94.3	.46	48.3	.83	61.3	ISOPAC #6
" 22	.76	59	1.31	78.3	1.54	86	1.69	91.3	.42	47	.77	59.3	
" 23	.76	59	1.25	76	1.47	83.7	1.56	87	.41	46.7	.71	57.3	HOT PLATE
" 24	.76	59	1.30	78	1.53	85.7	1.65	90	.41	46.7	.74	58.3	
" 25	.75	58.7	1.30	78	1.53	85.7	1.68	91	.40	46.3	.74	58.3	
" 26	.76	59	1.32	78.7	1.56	87	1.71	92	.40	46.3	.77	59.3	
" 27	.76	59	1.31	78.3	1.54	86	1.68	91	.42	47	.77	59.3	
" 28	.70	57	1.07	70	1.18	73.7	1.22	75	.32	43.3	.48	49	THERMAL CONTROL HEAT PIPES
" 29	.77	59.3	1.12	71.7	1.22	75	1.25	76	.42	47	.57	52.3	
" 30	.72	57.7	1.06	69.7	1.19	74	1.23	75.3	.34	44	.50	50	
" 31	.77	59.3	1.13	72	1.24	75.7	1.27	76.7	.42	47	.59	53	
" 32	.70	57	1.06	69.7	1.17	73.3	1.21	74.7	.32	43.3	.46	48.3	

(SHEET #2)

1	2	3	4	5	6	7	8	9	10	11	12	13	14	15	16	17	18	19	20	21	22	23	24	25	26	27	28	29	30	31	32	33	34	35	36	37	38	39	40	41	42	43	44	45	46	47	48	49	50	51	52	53	54	55	56	57	58	59	60	61	62	63	64	65	66	67	68	69	70	71	72	73	74	75	76	77	78	79	80	81	82	83	84	85	86	87	88	89	90	91	92	93	94	95	96	97	98	99	100
---	---	---	---	---	---	---	---	---	----	----	----	----	----	----	----	----	----	----	----	----	----	----	----	----	----	----	----	----	----	----	----	----	----	----	----	----	----	----	----	----	----	----	----	----	----	----	----	----	----	----	----	----	----	----	----	----	----	----	----	----	----	----	----	----	----	----	----	----	----	----	----	----	----	----	----	----	----	----	----	----	----	----	----	----	----	----	----	----	----	----	----	----	----	----	----	----	----	----	-----



# PITCH PERFORMANCE TESTS

## (SHEET #1)

	PERFORMANCE TEST RUNS												
	# 7		# 8		# 9		# 10		# 11		# 12		
DATE	4-13-71		4-9-71		4-5-71		4-5-71		4-6-71		4-14-71		COMMENTS
TIME	8:35		15:10		11:25		15:35		12:00		13:15		
POWER	100W		125W		0W		75W		100W		100W		
BATH TEMP	-4°F		-4°F		68°F		68°F		68°F		-4°F		
BATTERY PRESSURE	40#/in <sup>2</sup>		40#/in <sup>2</sup>		40#/in <sup>2</sup>		40#/in <sup>2</sup>		40#/in <sup>2</sup>		40#/in <sup>2</sup>		
T/C #1	1.35	79.7	1.56	87	1.22	75	1.93	99.7	2.11	105.7	1.68	91	BATTERY #1
" 2	1.35	79.7	1.56	87	1.22	75	1.94	100	2.11	105.7	1.68	91	
" 3	1.41	81.7	1.65	90	1.22	75	1.98	101.3	2.18	108.3	1.75	93.3	BATTERY #2
" 4	1.42	82	1.65	90	1.22	75	1.98	101.3	2.18	108.3	1.75	93.3	
" 5	1.48	84	1.72	93.3	1.22	75	2.01	102.3	2.24	110.3	1.79	94.7	BATTERY #3
" 6	1.48	84	1.73	92.7	1.22	75	2.01	102.3	2.24	110.3	1.79	94.7	
" 7	1.49	84.3	1.73	92.7	1.22	75	2.01	102.3	2.24	110.3	1.79	94.7	BATTERY #4
" 8	1.49	84.3	1.74	93	1.22	75	2.01	102.3	2.24	110.3	1.79	94.7	
" 9	1.46	83.3	1.70	91.7	1.22	75	2.00	102	2.18	108.3	1.76	93.7	BATTERY #5
" 10	1.46	83.3	1.70	91.5	1.22	75	1.99	101.7	2.18	108.3	1.76	93.7	
" 11	1.25	76	1.43	82.3	1.22	75	1.86	97.3	2.00	102	1.59	88	ISOPAC #1
" 12	1.16	73	1.32	78.7	1.22	75	1.80	95	1.93	99.7	1.51	85	
" 13	1.33	79	1.54	86	1.22	75	1.92	99.3	2.10	105.3	1.66	90.3	ISOPAC #2
" 14	1.22	75	1.40	81.3	1.22	75	1.84	96.5	1.99	101.7	1.56	87	
" 15	1.40	81.3	1.62	89	1.22	75	1.95	100.3	2.15	107.3	1.72	92.3	ISOPAC #3
" 16	1.26	76.3	1.46	83.3	1.22	75	1.86	97.3	2.03	103	1.59	88	
" 17	1.43	82.3	1.67	90.7	1.22	75	1.97	101	2.18	108.3	1.74	93	ISOPAC #4
" 18	1.29	77.3	1.49	84.3	1.22	75	1.87	97.7	2.06	104	1.61	88.7	
" 19	1.42	82	1.64	89.7	1.22	75	1.97	101	2.16	107.7	1.73	92.7	ISOPAC #5
" 20	1.30	78	1.49	84.3	1.22	75	1.87	97.7	2.04	103.3	1.61	88.7	
" 21	1.36	80	1.56	87	1.23	75.3	1.91	99	2.06	104	1.66	90.3	ISOPAC #6
" 22	1.27	76.7	1.46	83.3	1.23	75.3	1.85	97	2.00	102	1.59	88	
" 23	1.15	72.7	1.31	78.3	1.22	75	1.79	94.7	1.92	99.3	1.50	84.7	HOT PLATE
" 24	1.23	75.3	1.42	82	1.22	75	1.84	96.5	2.00	102	1.57	87.3	
" 25	1.25	76	1.45	83	1.22	75	1.85	97	2.02	102.7	1.57	87.3	
" 26	1.29	77.3	1.48	84	1.22	75	1.87	97.7	2.04	103.3	1.60	88.3	
" 27	1.27	76.7	1.46	83.3	1.22	75	1.85	97	2.00	102	1.58	87.7	
" 28	.83	61.5	.90	64	1.22	75	1.56	87	1.62	89	1.24	75.7	THERMAL CONTROL HEAT PIPES
" 29	.87	63	.92	64.7	1.22	75	1.60	88.3	1.66	90.3	1.24	75.7	
" 30	.84	62	.91	64.3	1.22	75	1.57	87.3	1.63	89.3	1.24	75.7	
" 31	.88	63.3	.93	65	1.22	75	1.62	89	1.68	91	1.27	76.7	
" 32	.82	61	.89	63.7	1.20	74.3	1.55	86.5	1.61	88.7	1.23	75.3	



(SHEET #2)

[illegible]

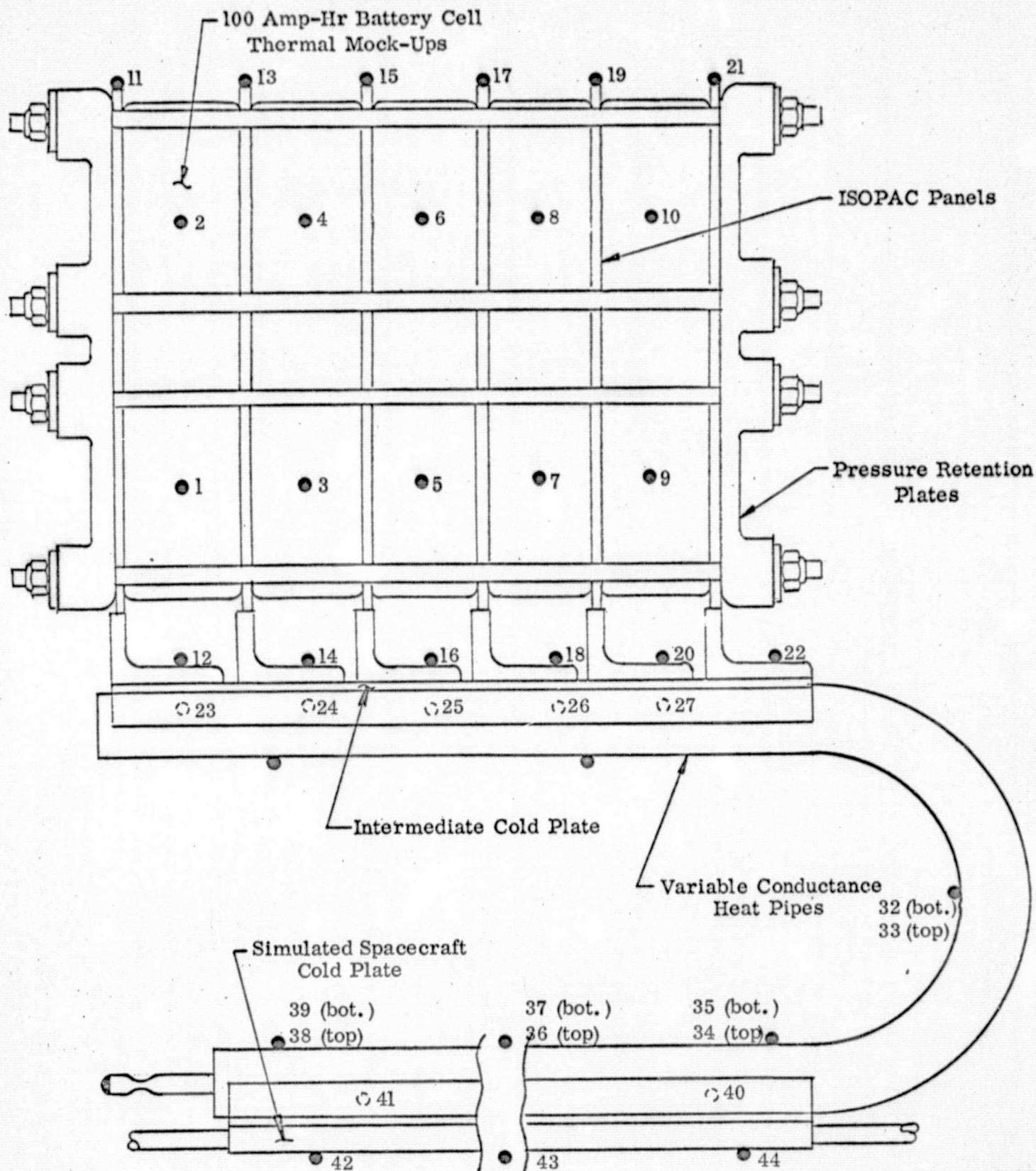
(SHEET # 1)

	PERFORMANCE TEST RUNS						
	# 13	#	#	#	#	#	
DATE	4-14-71						COMMENTS
TIME	16:40						
POWER	100W						
BATH TEMP	32°F						
BATTERY PRESSURE	90 <sup>psi</sup> /in <sup>2</sup>						
T/C #1	1.96 100.7						{ BATTERY #1
" 2	1.96 100.7						
" 3	2.02 102.7						
" 4	2.02 102.7						
" 5	2.06 104						
" 6	2.06 104						{ BATTERY #2
" 7	2.06 104						
" 8	2.07 104.3						
" 9	2.01 102.3						
" 10	2.02 102.7						
" 11	1.86 97.3						{ BATTERY #3
" 12	1.79 94.7						
" 13	1.94 100						
" 14	1.84 96.3						
" 15	1.99 101.7						
" 16	1.86 97.3						{ BATTERY #4
" 17	2.01 102.7						
" 18	1.88 98						
" 19	1.99 101.7						
" 20	1.88 98						
" 21	1.92 99.3						{ BATTERY #5
" 22	1.85 97						
" 23	1.78 94.3						
" 24	1.84 96.3						
" 25	1.84 96.3						
" 26	1.87 97.7						{ ISOPAC #1
" 27	1.85 97						
" 28	1.55 86.5						
" 29	1.56 87						
" 30	1.56 87						
" 31	1.58 87.7						{ ISOPAC #2
" 32	1.54 86						
							{ ISOPAC #3
							{ ISOPAC #4
							{ ISOPAC #5
							{ ISOPAC #6
							{ HOT PLATE
							{ THERMAL CONTROL HEAT PIPES



(SHEET #2)

[illegible]



LOCATION OF TEST INSTRUMENTATION

APPENDIX B

**PERFORMANCE TEST SUMMARY**



# PERFORMANCE TEST SUMMARY

COOLANT TEMPERATURE =  $-4^{\circ}\text{F}$

BATTERY PRESSURE =  $40^{\#}/\text{in}^2$

BATTERY POWER (WATTS)	AVERAGE CELL TEMP ( $^{\circ}\text{F}$ )	AVERAGE ISOPAL TEMP ( $^{\circ}\text{F}$ )	AVERAGE HOT PLATE TEMP ( $^{\circ}\text{F}$ )	AVERAGE VARIABLE CONDUCTANCE HEAT PIPE TEMPERATURE ( $^{\circ}\text{F}$ )				AVERAGE COLD PLATE TEMP ( $^{\circ}\text{F}$ )	AVERAGE CHILL PLATE TEMP ( $^{\circ}\text{F}$ )
				EVAP SECT	TRANS SECT	COND. SECT.	STORAGE VOLUME		
0	47.2	47.2	46.6	43.6 47	43.3 47	6.0 5.2	3.0 7.7	2.8	1.2
50	62.6	60.0	58.5	49.5 52.6	48.3 52.3	26.5 26.9	4.7 8.7	11.2	4.8
100	82.6	78.1	75.6	61.7 63.1	61.0 63.0	34.6 35.8	6.5 10.7	18.1	8.7
125	90.8	85.0	82.1	64.1 64.8	63.7 64.3	38.0 37.7	6.0 10.7	20.5	11.2

# PERFORMANCE TEST SUMMARY

COOLANT TEMPERATURE = 32°F

BATTERY PRESSURE = 40 <sup>#</sup>/in<sup>2</sup>

BATTERY POWER (WATTS)	AVERAGE CELL TEMP (°F)	AVERAGE ISOPAL TEMP (°F)	AVERAGE HOT RATE TEMP (°F)	AVERAGE VARIABLE CONDUCTANCE HEAT PIPE TEMPERATURE (°F)				AVERAGE COLD RATE TEMP (°F)	AVERAGE CHILL PLATE TEMP (°F)
				EVAP SECT	TRANS SECT	COND. SECT.	STORAGE VOLUME		
0	59.4	59.4	58.9	57.3 59.3	57.0 59.0	36.0 35.5	34.0 36.7	33.6	33.6
75	82.0	78.8	76.9	65.5 67.6	64.7 67.3	50.8 52.3	36.0 38.0	41.5	37.1
100	92.5	87.9	85.6	75.1 76.3	74.7 75.7	59.1 58.3	36.0 38.0	44.5	39.2
125	98.5	93.0	90.2	73.8 75.3	73.3 75.0	56.3 57.1	36.7 39.0	45.0	39.7

## PERFORMANCE TEST SUMMARY

COOLANT TEMPERATURE =  $68^{\circ}\text{F}$

BATTERY PRESSURE = 40 #/IN<sup>2</sup>

[illegible]



# PERFORMANCE TEST SUMMARY

COOLANT TEMPERATURE =  $-4^{\circ}\text{F}$

BATTERY PRESSURE =  $40^{\frac{\text{psi}}{\text{in}^2}}$

BATTERY POWER (WATTS)	AVERAGE CELL TEMP ( $^{\circ}\text{F}$ )	AVERAGE ISOPAL TEMP ( $^{\circ}\text{F}$ )	AVERAGE HOT PLATE TEMP ( $^{\circ}\text{F}$ )	AVERAGE VARIABLE CONDUCTANCE HEAT PIPE TEMPERATURE ( $^{\circ}\text{F}$ )				AVERAGE COLD PLATE TEMP ( $^{\circ}\text{F}$ )	AVERAGE CHILL PLATE TEMP ( $^{\circ}\text{F}$ )
				EVAP SECT	TRANS SECT	COND. SECT.	STORAGE VOLUME		
* 100	93.5	89.3	87.1	75.7 76.2	75.3 75.3	42.3 43.0	74.0 74.7	20.0	11.6

\* AUXILIARY POWER INPUT OF 15 WATTS  $\pm$  12.3 WATTS TO  
HEATERS ON VARIABLE CONDUCTANCE HEAT PIPE  
STORAGE VOLUMES.

# PERFORMANCE TEST SUMMARY

COOLANT TEMPERATURE = 32 °F

BATTERY PRESSURE = 40 #/IN.<sup>2</sup>

BATTERY POWER (WATTS)	AVERAGE CELL TEMP (°F)	AVERAGE ISOPAL TEMP (°F)	AVERAGE HOT RATE TEMP (°F)	AVERAGE VARIABLE CONDUCTANCE HEAT PIPE TEMPERATURE (°F)				AVERAGE COLD RATE TEMP (°F)	AVERAGE SHILL PLATE TEMP (°F)
				EVAP SECT	TRANS SECT	COND. SECT.	STORAGE VOLUME		
* 100	102.8	98.6	96.3	86.7 87.3	86.0 87.3	61.5 62.1	85.0 86.0	44.8	39.1

\* AUXILIARY POWER INPUT OF 15 WATTS & 12.3 WATTS TO HEATERS  
ON VARIABLE CONDUCTANCE HEAT PIPE STORAGE  
VOLUMES.